Flexible Interoperable Transceiver (FIT) Program Test Range II: Radio Propagation Measurements at 440, 1360 and 1920 MHz Ft. Hood, Texas

Peter Papazian
Perry Wilson
Michael Cotton
Yeh Lo

U.S. DEPARTMENT OF COMMERCE
Norman Y. Mineta, Secretary

Gregory L. Rohde, Assistant Secretary
for Communications and Information

October 2000

This Page Intentionally Left Blank

Disclaimer

Certain commercial equipment and materials are identified in this report to specify adequately the technical aspects of the reported results. In no case does such identification imply recommendations or endorsement by the National Telecommunications and Information Administration, nor does it imply that the material or equipment identified is the best available for this purpose.

This Page Intentionally Left Blank

This Page Intentionally Left Blank

CONTENTS

This Page Intentionally Left Blank

This Page Intentionally Left Blank

EXECUTIVE SUMMARY

This report describes mobile communication link measurements made at Ft. Hood, Coryell County, Texas, in support of the Flexible Interoperable Transceiver (FIT) program. Ft. Hood is the second of four locations measured, the other three being Edwards Air Force Base, CA (completed), Fort Polk, LA (pending) and Camp Lejeune, NC (pending). The goal of the measurement series is to define communication link characteristics at different frequencies over a representative cross section of military training centers.

The measurements were made using the Institute for Telecommunication Sciences (ITS) multiple channel impulse response system (see Report, Section 3). The primary figures of merit used to characterize wireless communication links are basic transmission loss (L_{BT}) and delay statistics. Three frequencies were considered: 440 MHz, 1360 MHz, and 1920 MHz. 440 MHz is representative of several current ground-to-ground communication links (JRTC-IS, PRIME, PLRS). 1360 MHz is proposed for the next generation FIT system. 1920 MHz has similar characteristics to the 1710-1850 MHz band, which is also under consideration for FIT. By comparing the 1360 MHz and 1920 MHz basic transmission loss and delay statistics to those for 440 MHz, the viability of using higher frequencies for future military communications and the associated system requirements can be assessed. At Ft. Hood a second 1360 MHz receiver channel was added. This channel was used to monitor a "low" 1360 MHz receive antenna. The purpose of this experiment was to measure the difference in received signal using a hand held "low" antenna (ground soldier) versus a vehicle-mounted antenna. As before, all channels are measured simultaneously.

Two transmitter sites and a common receiver vehicle route were selected. At both transmit sites the antennas were elevated using a 10-m mast on a Humvee provided by TEXCOM. Site 1 was located on Anderson Mountain directly north of Copperas Cove. Ground elevation at this site is 360 m. The transmitter elevation including mast was 370 m. This site had a view of the training range to the ridge-line of the Manning Mountains just north of the Manning Mountains Road. In general, Anderson Mountain had good views of the range except when obscured by vegetation (cypress trees) or valleys cut by streams. Some of these obstructions would presumably not exist for the second transmit site at Pidcoke. Pidcoke (Site 2) is located near the intersection of Antelope Road and the State Highway, which forms the western boundary of the Military Reservation. The elevation at Pidcoke is approximately 275 m. The 10-m Humvee mast was used to place the antennas at 285 m elevation. Photographs and maps of the transmitter and receiver locations are in the figures from Section 2 of the report.

Data were collected simultaneously at three frequencies. The major question answered by the survey is the effect of frequency translation on radio propagation parameters. To quantify propagation impairments caused by frequency translation, the impulse response data were analyzed and the following metrics tabulated:

1. Linear curve fit parameters n (path loss exponent) and B (multiplier) are tabulated for basic transmission loss (L_{BT}) versus distance for three frequencies. The path loss exponent, n, is the critical parameter. For line of sight propagation with loss only due to signal spreading (free space loss, L_{FS}), $n = 2$. In areas with obstructions caused by terrain, vegetation, or buildings, n typically varies between 2 and 4 due to diffraction, attenuation and multipath interference. Column 1, Tables ES1 and ES2 summarize the n and B parameters (see Report, Section 4 for more details). By substituting these parameters into the curve fit equation, a best fit approximation of path loss versus distance can be calculated for the different frequencies and transmitters. These curves are then used in conjunction with the free space loss curve to determine additional loss over free space ($\Delta L_{BT/FS}$). They are also used to determine signal loss due to frequency translation from 440 MHz to higher frequencies ($\Delta L_{BT/440}$).

2. The difference between the linear fit estimates and ideal free space values is designated $\Delta L_{BT/FS}$. These data indicate the additional loss over the basic free space loss. The $\Delta L_{BT/FS}$ data range is approximately 15 to 30 dB for Anderson Mountain and 20 to 40 dB for Pidcoke. This difference is most likely due to the transmitter elevations. The Anderson Mountain transmitter was at an elevation of 370 m which is about 120 m above the survey area. The Pidcoke transmitter was at an elevation of 285 m or about 35 m above the survey area. This difference compares to a $\Delta L_{BT/FS}$ range of 10 to 20 dB for the high transmitter at Edwards Air Force Base (EAFB) and 20 to 40 dB for the low transmitter at EAFB. At EAFB the low transmitter was only 5 m above the survey area, while the high transmitter was also 120 m above the survey area. At Ft. Hood the high unobstructed transmitter (Anderson Mountain) had a larger $\Delta L_{BT/FS}$ than the high transmitter at EAFB and a slightly smaller loss than the obstructed low transmitter at EAFB. The received signal from Pidcoke was about equal with the received signal from the lower transmitter at EAFB. The additional losses versus distance for these higher transmitters at Ft. Hood are most likely due to obstructions caused by vegetation and terrain. Tables ES1 and ES2 and Report, Section 4 summarize these data for Ft. Hood.

3. The difference between the 1360 and 1920 MHz linear fit estimates and the 440 MHz linear fit estimate is designated $\Delta L_{BT/440}$. These numbers can be used to determine the extra transmit power, system sensitivity, diversity gain, or BER versus signal to noise requirements of the proposed higher frequency systems. The $\Delta L_{BT/440}$ data range over approximately 7 to 12 dB for the 1360 MHz van roof data and 11 to 15 dB for the 1920 MHz data. For this metric there is no noticeable difference between the two transmitter sites (see Tables ES1 and ES2 and Report, Section 4). For comparison, the $\Delta L_{BT/440}$ data for EAFB varies from 5 to 15 dB for the 1360 MHz data and 10 to 20 dB for the 1920 MHz data. So we see that there is 3 to 5 dB less differential loss due to frequency translation at Ft. Hood than at EAFB.

4. An alternative to curve fitting the measured data is to bin the L_{BT} data. This is done versus distance, and the mean and standard deviation for each bin are calculated as well as the 90% and 99% probability levels (i.e. 99% of the L_{BT} data are less than this level). 99% L_{BT} levels range from 98 to 167 dB for Anderson Mountain and from 105

to 167 dB for Pidcoke. The larger values were limited by the dynamic range of the measurement system. The maximum range before this limit was reached using the 1360 MHz high receiver was about 15 km for Anderson Mountain and about 10 km for Pidcoke. These data give the upper bounds for the measured transmission loss L_{BT} and indicate maximum signal loss on the link required to ensure a certain channel availability probability (see Tables ES3 and ES4 and Report, Section 4). The difference between the mean and the 99% level can also be added to the curve fit to extend the curve fit requirements to the 99% availability level. 99% L_{BT} levels ranged from 126 to 163 dB in Cell 1 (low transmitter) at EAFB and from 117 to 157 dB in Cell 2 (high transmitter) at EAFB.

5. Delay statistics are necessary for design of a digital system. They are used to determine equalizer requirements for elimination of inter-symbol interference. In general, delay increases with frequency and with the presence of scattering objects (low transmitter). Two figures of merit are the delay spread and the maximum delay. Tables ES5 through ES8 summarize the delay statistics for different probability levels. In these tables the maximum mean and delay spread are given versus frequency. For instance, at 90% probability, the maximum delay is 0.93 μs for both Anderson Mountain and Pidcoke at 440 MHz. At 1920 MHz and 90% probability, the maximum delay ranges between 1.18 μs at Pidcoke down to 0.65 μs at Anderson Mountain. These data are based on average power delay profiles (APDPs) with a 20 dB interval of discrimination (ID). A 20 dB ID means that the impulse peak to noise is > 23 dB and only echoes within 20 dB of the peak are included in the statistics, see Report, Section 5 for more details). For comparison, the delay spreads at EAFB are up to 2.2 μs for 440 MHz and up to 4.1 μs for 1920 MHz. We see a decrease in multipath at Ft. Hood versus EAFB that probably is due to the lack of large metal hangers and multistory office buildings in the training area at Ft. Hood. The few buildings seen while driving the range at Ft. Hood were a small mock village which appeared to consist only of wooden buildings.

6. Simultaneous impulse response measurements at 1360 MHz were made using two receive antennas placed at different heights. This experiment was designed to measure possible signal degradation between higher vehicle-mounted antennas and lower antennas carried by foot soldiers. The low antenna was approximately 0.5 m above the ground and towed behind the recording vehicle. The high antenna was 2.5 m above the ground and situated on the van roof. Measurements indicated that the low antenna suffered a 2 to 3 dB decrease in average received signal strength. These results were determined using curve fitting (see Report, Section 4 and Figures 4.19 and 4.20).

Table ES1. Curve Fit Parameters, Free Space Loss and 440 MHz Loss Compared to Basic Transmission Loss Collected Using Anderson Mountain Transmitter Site

| F (MHz) | L_{BT} Linear Fit Parameters | | Distance (km) | | | | | |
| | | | 2.0 | | | 20 | | |
	n	B (km^{-1})	L_{FS} (dB)	$\Delta L_{BT/FS}$ (dB)	$\Delta L_{BT/440}$ (dB)	L_{FS} (dB)	$\Delta L_{BT/FS}$ (dB)	$\Delta L_{BT/440}$ (dB)
440	3.3	848	91.3	15.6	N/A	111.3	28.7	N/A
1360	3.5	1010	101.1	15.8	10.1	121.1	31.3	12.4
1920	3.1	4107	104.1	16.4	13.7	124.1	27.3	11.4

Table ES2. Curve Fit Parameters, Free Space Loss and 440 MHz Loss Compared to Basic Transmission Loss Collected Using Pidcoke Transmitter Site

| F (MHz) | L_{BT} Linear Fit Parameters | | Distance (km) | | | | | |
| | | | 1.0 | | | 10.0 | | |
	n	B (km^{-1})	L_{FS} (dB)	$\Delta L_{BT/FS}$ (dB)	$\Delta L_{BT/440}$ (dB)	L_{FS} (dB)	$\Delta L_{BT/FS}$ (dB)	$\Delta L_{BT/440}$ (dB)
440	3.4	1451	85.3	22.2	N/A	105.3	36.2	N/A
1360	3.9	854	95.1	19.5	7.1	115.1	38.6	12.2
1920	3.1	9932	104.1	24.2	14.8	118.1	34.8	11.4

Table ES3. Anderson Mt. Basic Transmission Loss (L_{BT}): Free Space Loss (L_{FS}) and Measured Mean (Avg), 90%, and 99% Probability Levels

| D (km) | L_{FS} (dB) | L_{BT} (dB): 440 MHz | | | L_{FS} (dB) | L_{BT} (dB): 1360 MHz (trailer) | | | L_{FS} (dB) | L_{BT} (dB): 1360 MHz (van) | | | L_{FS} (dB) | L_{BT} (dB): 1920 MHz | | |
		Avg	90%	99%		Avg	90%	99%		Avg	90%	99%		Avg	90%	99%
0.7	82.8	92.2	96.9	98.8	92.6	106.0	120.7	125.3	92.6	104.3	114.6	119.6	95.6	105.6	110.4	112.6
1.8	90.3	106.8	113.9	114.1	100.1	117.7	125.8	126.3	100.1	116.2	119.7	120.1	103.1	123.9	127.1	128.4
2.8	94.2	110.1	120.3	122.1	104.0	121.9	130.0	133.2	104.0	121.1	132.6	138.2	107.0	125.6	137.6	139.1
3.8	96.9	112.5	126.5	130.3	106.7	128.1	144.9	149.9	106.7	125.2	145.1	152.7	109.7	127.8	144.1	148.9
4.8	99.0	119.8	125.2	127.1	108.8	135.6	147.5	156.5	108.8	136.4	152.9	160.7	111.8	137.6	146.6	155.8
5.8	100.6	120.2	131.3	137.2	110.4	135.8	152.0	159.0	110.4	131.5	150.3	155.9	113.4	132.5	149.6	154.2
6.9	102.0	127.2	142.1	145.0	111.8	141.7	165.7	166.8	111.8	141.9	165.2	166.4	114.8	144.3	161.9	164.3
7.9	103.2	121.3	129.6	138.1	113.0	136.8	151.7	162.5	113.0	128.8	142.2	161.1	116.0	130.0	141.7	150.7
8.9	104.3	129.9	140.7	146.3	114.1	145.8	159.7	165.9	114.1	141.7	162.7	166.0	117.1	140.6	156.1	161.3
9.9	105.2	131.0	135.4	138.5	115.0	145.1	154.7	160.5	115.0	142.8	154.3	162.1	118.0	142.5	149.9	155.0
10.9	106.1	148.5	156.2	158.2	115.9	161.3	166.6	167.3	115.9	162.6	166.2	166.9	118.9	158.8	165.9	166.9
12.0	106.9	147.3	159.3	160.7	116.7	160.8	166.7	167.3	116.7	159.5	166.4	167.1	119.7	158.6	166.4	167.1
13.0	107.6	140.3	149.9	158.0	117.4	157.5	166.3	167.2	117.4	158.0	165.9	166.9	120.4	156.9	165.7	166.7
14.0	108.2	136.2	144.5	151.1	118.0	151.8	164.5	166.7	118.0	151.7	165.2	166.3	121.0	147.9	159.0	164.1
15.0	108.8	134.8	157.3	159.3	118.6	154.1	166.6	167.5	118.6	142.7	166.4	167.2	121.6	144.0	166.2	167.1
16.0	109.4	129.2	145.2	158.6	119.2	141.0	161.5	166.7	119.2	140.0	164.9	166.5	122.2	140.6	160.6	166.5
17.1	110.0	132.6	151.3	153.9	119.8	154.7	166.0	167.1	119.8	149.6	165.8	166.8	122.7	147.2	165.5	166.7
18.1	110.5	131.5	144.8	151.4	120.3	149.0	165.8	167.1	120.3	147.7	165.6	166.6	123.3	146.3	163.4	165.9
19.1	110.9	142.4	150.8	152.8	120.7	160.3	166.7	167.3	120.7	157.6	166.3	167.0	123.7	154.7	166.3	166.9
20.1	111.4	145.2	158.5	160.2	121.2	159.4	166.7	167.5	121.2	159.9	166.3	167.0	124.2	157.9	166.3	167.0

Table ES4. Pidcoke Basic Transmission Loss (L_{BT}): Free Space Loss (L_{FS}) and Measured Mean (Avg), 90%, and 99% Probability Levels

D (km)	L_{FS} (dB)	L_{BT} (dB): 440 MHz			L_{FS} (dB)	L_{BT} (dB): 1360 MHz (trailer)			L_{FS} (dB)	L_{BT} (dB): 1360 MHz (van)			L_{FS} (dB)	L_{BT} (dB): 1920 MHz		
		Avg	90%	99%		Avg	90%	99%		Avg	90%	99%		Avg	90%	99%
0.3	75.1	92.2	97.1	105.6	84.9	107.6	113.9	124.9	84.9	108.1	116.7	125.1	87.9	109.2	120.5	126.5
0.7	81.7	107.4	114.0	119.4	91.5	121.8	127.9	130.0	91.5	111.2	122.0	126.6	94.5	115.1	129.8	134.4
1.0	85.4	106.3	114.6	116.2	95.2	122.6	127.2	128.7	95.2	114.5	124.4	126.3	98.2	118.2	128.1	130.6
1.4	87.9	111.4	114.3	115.1	97.7	129.5	134.9	138.8	97.7	116.1	119.6	126.7	100.7	120.9	129.0	136.8
2.0	91.5	130.3	143.4	150.8	101.3	153.4	166.4	167.4	101.3	148.6	165.4	166.5	104.3	150.4	165.9	166.9
3.1	95.1	113.7	124.4	128.4	104.9	138.4	144.8	151.2	104.9	128.4	142.7	146.2	107.9	130.6	141.0	146.7
4.1	97.6	130.2	149.9	155.4	107.4	145.5	158.7	164.6	107.4	143.7	164.0	165.9	110.4	141.8	156.0	161.2
5.2	99.6	122.4	128.8	135.4	109.4	140.3	155.1	160.3	109.4	133.6	145.2	154.9	112.4	133.6	142.9	154.1
6.2	101.2	131.8	140.4	143.4	111.0	146.7	157.8	165.2	111.0	144.1	159.9	166.2	114.0	143.0	155.2	163.8
7.3	102.5	131.4	151.1	155.4	112.3	141.5	165.7	167.2	112.3	139.6	166.0	166.9	115.3	142.4	165.3	166.9
8.0	103.3	133.7	144.2	146.8	113.1	147.6	164.6	167.1	113.1	147.9	165.5	166.6	116.1	146.0	160.4	166.2
9.0	104.4	139.6	155.2	157.0	114.2	158.1	166.9	167.7	114.2	158.2	166.2	166.9	117.2	153.8	166.3	167.2
10.1	105.4	152.5	157.5	158.9	115.2	165.0	167.5	168.1	115.2	164.8	166.6	167.2	118.2	164.1	167.1	167.7
11.1	106.2	150.8	156.5	158.1	116.0	164.5	167.3	167.9	116.0	164.9	166.5	167.1	119.0	162.7	166.9	167.7
12.1	107.0	140.9	148.1	151.3	116.8	159.8	166.4	167.5	116.8	157.4	166.0	166.9	119.8	150.3	165.0	167.2
13.2	107.7	146.5	156.8	158.8	117.5	159.2	167.2	168.2	117.5	161.4	166.5	167.1	120.5	157.0	166.7	167.5
13.9	108.2	142.9	151.4	156.3	118.0	157.4	166.0	167.5	118.0	160.8	165.8	167.0	121.0	154.0	164.5	166.7

Table ES5. Anderson Mt.: Delay Statistics for APDPs with a 20 dB ID

	440 MHz			1360 MHz (Trailer)			1360 MHz (Van)			1920 MHz		
	69 % APDPs Valid			52 % APDPs Valid			52 % APDPs Valid			61 % APDPs Valid		
Prob. (%)	Delay (µs)			Delay (µs)			Delay (µs)			Delay (µs)		
	max	avg	spr	max	avg	spr	max	avg	spr	max	avg	spr
90.0	0.93	0.15	0.15	0.75	0.15	0.13	0.55	0.13	0.08	0.65	0.13	0.09
99.0	17.4	1.52	3.92	12.1	1.26	2.59	14.7	1.57	3.48	12.0	1.78	3.35
99.9	23.1	17.8	7.03	39.3	22.1	9.21	20.8	17.4	6.06	24.3	18.4	8.30

Table ES6. Anderson Mt.: Delay Statistics for APDPs with a 10 dB ID

	440 MHz			1360 MHz (Trailer)			1360 MHz (Van)			1920 MHz		
	81 % APDPs Valid			69 % APDPs Valid			67 % APDPs Valid			74 % APDPs Valid		
Prob. (%)	Delay (µs)			Delay (µs)			Delay (µs)			Delay (µs)		
	max	avg	spr	max	avg	spr	max	avg	spr	max	avg	spr
90.0	0.13	0.09	0.03	0.23	0.11	0.06	0.15	0.09	0.03	0.15	0.09	0.04
99.0	1.65	0.30	0.46	9.43	3.25	3.03	2.33	0.72	0.74	7.15	3.71	3.08
99.9	7.13	1.84	2.30	23.7	10.5	8.59	10.9	7.02	3.55	23.7	8.69	9.15

Table ES7. Pidcoke: Delay Statistics for APDPs with a 20 dB ID

Prob. (%)	440 MHz			1360 MHz (Trailer)			1360 MHz (Van)			1920 MHz		
	60 % APDPs Valid			43 % APDPs Valid			42 % APDPs Valid			56 % APDPs Valid		
	Delay (µs)			Delay (µs)			Delay (µs)			Delay (µs)		
	max	avg	spr	max	avg	spr	max	avg	spr	max	avg	spr
90.0	0.93	0.16	0.14	0.75	0.16	0.12	0.56	0.14	0.09	1.18	0.18	0.19
99.0	9.70	1.14	2.26	10.2	1.94	2.59	3.48	0.40	0.77	7.25	0.93	1.67
99.9	17.5	3.89	5.40	19.0	3.21	5.39	18.9	1.32	3.78	10.9	2.56	2.77

Table ES8. Pidcoke: Delay Statistics for APDPS with a 10 dB ID

Prob. (%)	440 MHz			1360 MHz (Trailer)			1360 MHz (Van)			1920 MHz		
	76 % APDPs Valid			60 % APDPs Valid			59 % APDPs Valid			69 % APDPs Valid		
	Delay (µs)			Delay (µs)			Delay (µs)			Delay (µs)		
	max	avg	spr	max	avg	spr	max	avg	spr	max	avg	spr
90.0	0.13	0.09	0.03	0.30	0.13	0.07	0.18	0.10	0.04	0.18	0.10	0.04
99.0	2.10	0.75	0.88	5.88	2.73	2.21	2.18	0.64	0.72	3.48	0.88	1.17
99.9	9.73	2.93	3.69	14.5	5.49	4.97	7.58	1.96	2.59	13.5	5.52	4.69

LIST OF FIGURES

Page

LIST OF TABLES

FLEXIBLE INTEROPERABLE TRANSCEIVER (FIT) PROGRAM TEST RANGE II: RADIO PROPAGATION MEASUREMENTS AT 440, 1360 AND 1920 MHz, FT. HOOD, TEXAS

Peter Papazian, Perry Wilson, Michael Cotton and Yeh Lo[*]

Radiowave propagation measurements at Ft. Hood, Texas are described. These measurements were made as part of the Flexible Interoperable Transceiver (FIT) Program. The objective of the measurements is to define communication link requirements at 440, 1360, and 1920 MHz. Simultaneous wideband measurements at three frequencies were made using fixed transmitters and a mobile fitted with a multi-channel receiver. The system measured the radio channel impulse response. Data outputs include delay spread and basic transmission loss. These parameters are compared at the three measurement frequencies to determine additional propagation impairments military systems will suffer due to frequency translation from 440 MHz to 1360 MHz and 1920 MHz.

Key Words: impulse response; radiowave propagation; Flexible Interoperative
Transceiver; FIT; delay spread; basic transmission loss.

1. INTRODUCTION

This report describes mobile communication link measurements made at Ft. Hood, Coryell County, Texas, in support of the Flexible Interoperable Transceiver (FIT) Program[**]. Ft. Hood is the second of four locations measured, the other three being Edwards Air Force Base, CA (completed), Fort Polk, LA (pending) and Camp Lejeune, NC (pending). The goal of the measurement series is to define communication link characteristics at different frequencies over a representative cross section of military training centers.

The primary figures of merit used to characterize wireless communication links are basic transmission loss and delay statistics. Basic transmission loss is the signal attenuation between the transmitting and receiving antennas due to path length, shadowing, and scattering. Basic transmission loss determines the range of the link if the transmit power and receiver sensitivity are known. The delay statistics quantify the signal power received over the direct, or shortest path (first arriving signal), versus the later multipath signals. Delay statistics are important in determining bit error rates and equalizer design.

Three frequencies are considered: 440 MHz, 1360 MHz, and 1920 MHz. 440 MHz is representative of several current ground to ground communication links (JRTC-IS, PRIME, PLRS). 1360 MHz is proposed for the next generation FIT system. 1920 MHz has similar characteristics to the 1710-1850 MHz band, which is also under consideration for FIT. By comparing the 1360 MHz and 1920 MHz basic transmission loss and delay statistics to those for 440 MHz, the viability of using higher frequencies for future military communications and the associated system requirements can be assessed. At Ft. Hood a second 1360 MHz receiver channel was added. This channel was used to monitor a "low" 1360 MHz receive antenna. The purpose of this experiment was to measure the difference in received signal using a hand held "low" antenna (ground soldier) versus a vehicle-mounted antenna. As before, all channels were measured simultaneously.

The report is organized as follows. Section 2 gives a brief description of the measurement site. Two transmitter locations were selected with one common drive route that covered the majority of the training area. Section 3 gives a brief overview of the Institute for Telecommunication Sciences (ITS) channel sounding system. The system uses a known pseudo-noise source that when received and processed closely approximates an ideal impulse signal over a wide bandwidth. Sections 4 and 5 detail the basic transmission loss measurements and delay statistics data. The figures are collected in Section 7. Appendices are included which detail antenna calibration and the effective isotropic radiated power (EIRP) utilized during the tests.

2. SITE DESCRIPTION

Ft. Hood is located in a rural area of central Texas north of Killeen, TX. The base is a principal U.S. Army training center for armored vehicle and tank crews. Its geography is defined by the soft, Cretaceous limestone sediments that create a hilly or hummocky terrain. The terrain is further broken up by numerous creek beds that have eroded small valleys in the surface rocks. These hills and valleys along with numerous cypress trees provide ample cover to hide tanks, as well as obstructions that adversely affect communications.

Two transmitter sites and a common receiver vehicle route were selected. At both transmit sites the antennas were elevated using a 10-m mast on a Humvee provided by TEXCOM. The mast had a 2 m spreader and the antennas were separated by approximately 1 m (see Figure 2.1). Site 1 was located on Anderson Mountain directly north of Copperas Cove. See Figure 2.2 for a view as seen from the transmitter. Ground elevation at this site is 360 m. The transmitting antenna elevation including mast was 370 m. GPS coordinates of the transmitter sites are listed in Appendix B. This site had a view of the training range to the ridge-line of the Manning Mountains just north of the Manning Mountains Road. Part of the drive route traverses the north side of the Manning Mountains near the Browns Creek Tank Range and on the West Range Road. In this area, the transmitted signal was obscured by terrain. This area was normally covered by the Owl Creek transmit site which was not used in this survey. In general, Anderson Mountain had good views of the range except when obscured by vegetation (cypress

trees) or valleys cut by streams. Some of these obstructions would presumably not exist for the second transmit site at Pidcoke. Pidcoke (Site 2) is located near the intersection of Antelope Road and the State Highway that forms the western boundary of the Military Reservation. The elevation at Pidcoke is approximately 275 m. The 10 m Humvee mast was used to place the antennas at 285 m elevation. Coverage from Pidcoke was also blocked to the NE by the Manning Mountains. Figure 2.3 shows the measurement van at Pidcoke with the trailer used for the low 1360 MHz antenna. Figure 2.4 gives another view at Pidcoke with the measurement crew. Maps showing the transmitter locations, drive routes and data file numbers are shown in Figures 2.5 and 2.6.

3. MEASUREMENT SYSTEM

The Institute for Telecommunication Sciences (ITS) antenna test bed (ATB) system used for these measurements is designed for measuring the radio channel impulse response. It can measure radio propagation parameters at multiple frequencies or from multiple antenna elements. It is used for the comparative testing of diversity schemes, adaptive antenna systems, and data processing algorithms. The key elements of the acquisition system are: 1) up to 8 simultaneous channels, 2) broadband channel impulse sounding, 3) high speed analog to digital data conversion and storage, and 4) flexible post processing. The multi-channel ATB sounder uses an upgraded version of the ITS digital channel probe (DCP). This probe has been used in previous programs (Motorola, USWEST, and PACTEL) to make impulse response measurements in the 900-MHz cellular and 1900-MHz PCS bands [1-3]. The system transmits a maximal-length pseudo noise (PN) code. The PN code is biphase shift key (BPSK) modulated onto an RF carrier. The transmitter is both frequency and bit-rate agile and can produce multiple PN codes and transmit frequencies simultaneously. The transmitted signal, modified by the radio channel, is received, down-converted to an intermediate frequency (IF), and then digitized. The impulse response is generated by cross correlating a copy of the transmitted PN code with the received signal after it has been converted to base band.

For the measurements reported here, the probe was configured to transmit a 511 bit PN word at 10 Mb/s on 440 MHz, 1360 MHz, and 1920 MHz carriers. The theoretical impulse signal to correlation noise ratio is 54 dB for a 511-bit PN sequence. The processing gain of the system is 27 dB. This means that when the signal power equals the noise power, the peak of the impulse response will be 27 dB above the noise. These parameters allow detection of multipath delays as great as 51 μs and resolution of multiple delays spaced as closely as 100 ns. Since the system measures the propagation time, the first arrival for signals traveling more than 16 km must be shifted in software so delayed signals will not wrap and appear to arrive first. This is easily done using the GPS coordinates and adding time offsets to the data at large transmitter-receiver separations. System timing is maintained using rubidium oscillators at the transmitter and receiver. These clocks synchronize the PN code generators, phase lock all local oscillators and provide sampling clocks for the digitizers. The oscillators' frequency stability ensures absolute timing measurements to within 50 ns for an 8-hour measurement period. It also allows measurement of the Doppler spectrum with 1 Hz accuracy. Data acquisition is

controlled by multiple digital signal processors (DSPs) and a host computer system. Acquisition was set to the burst mode for these tests. In this mode, a burst of data is collected in rapid sequence and stamped with GPS coordinates and time. The next data burst is acquired after a programmable delay that was set to 10 seconds for these measurements. Within a burst, the delay between impulses (51 μs in length) was set to 3 ms. The number of impulses per burst was set to 128. This resulted in an overall burst duration of approximately 388 ms. Table 1 summarizes the data acquisition parameters used for the diversity measurements, as well as the range of permissible values for the ATB system. Block diagrams for the system can be found in [4].

Mobile receiving antennas (RX) and fixed transmitting antennas (TX) were used. The transmitting antennas were mounted on a 10-m mast as described in Section 2. These antennas were omni-directional dipoles except for the 1360 MHz antenna. This antenna had an azimuthal pattern. A directional antenna pattern was utilized during the data processing by calculating the azimuth angle between the transmitter and receiver vehicle based on their GPS coordinates. The mobile receivers all used omni-directional monopole antennas. Three receiving antennas (440, 1360 and 1920 MHz) were mounted at a height of 2.4 m on the roof of a van equipped with a GPS/dead reckoning system. The fourth receive antenna was mounted on a trailer at an elevation of 0.5 m and towed behind the van. Receive antenna patterns and gains were measured in situ on the van and in an anechoic chamber using a 1.3 m diameter ground plane. An overview of the antenna characteristics is given in Table 2 (H = horizontal, V = vertical). For more detail on antenna calibrations see Appendix A.

The in-situ vertical plane antenna gain measurements were made in several locations in the far field using a clear line of sight. The measured data agree with manufacturer's specifications only for the 1360 and 1920 MHz transmitter antennas. Differences arise due to cables, connectors and environment. One important effect is that the van roof only approximates an infinite ground screen. This causes the vertical directivity of the receive antennas to peak near 20° [5]. Thus, along the horizon (0°) these antennas can have gains less than an isotropic radiator, as is the case for the 1360 and 1920 MHz receive antennas. To better quantify these effects, gain and directivity measurements were made in an anechoic chamber.

Table 1. ATB Data Acquisition and RF Parameters

Configurable System Parameters		
Parameter	Present Diversity Tests	ATB System
Receiver Channels	3	1-8
Carrier Frequencies	440, 1360, 1920 MHz	.45 – 6 GHz
Bit Rate	10 Mb/s	.1 – 50 Mb/s
Resolution	100 ns	10 μs – 20 ns
Code Type	Maximal Length	Programmable
Code Length	511 bits	Programmable
Acquisition Mode	Burst	Continuous or Burst
Positioning	GPS/Dead Reckoning	GPS/Dead Reckoning
Transmitters	3	Multiple
Data Processing	Post	Post or Real Time

Table 2. Overview of the Transmit and Receive Antenna Characteristics

Frequency	440 MHz	1360 MHz	1920 MHz
TX Antennas			
Type	Cushcraft FRX-430 Dipole	Dorne and Margolin DM Q130 -Dipole	Andrew PC1N0F-019A-006 Dipole
H-Plane Pattern	Omni-directional	Directional *	Omni-directional
V-Plane Gain (dBi)	1.7	11.3	6.9
RX Antennas		**see note	
Type	Larson 5/8λ monopole	Larson Base with ¼λ monopole	Andrew magmount PCS monopole
H-Plane Pattern	Omni-directional	Omni-directional	Omni-directional
V-Plane Gain (dBi)	1.2	-1.3	-0.7

* 160 degree 3-dB beamwidth, azimuth pattern from lookup table.
** Two 1360 MHz receive monopole antennas were used at the receiver. One was placed on the van roof, the second was positioned on a low trailer 0.5 m above the ground.

4. BASIC TRANSMISSION LOSS

Basic transmission loss (L_{BT}), is the signal attenuation between transmit and receive antennas due to free space, or spreading loss (L_{FS}), and signal attenuation. Basic transmission loss determines the range of the communications link. Basic transmission loss is given by

$$L_{BT}(dB) = P_t(dB) - P_r(dB) + G_t(dB) + G_r(dB) \qquad (4.1)$$

where P_t is the transmitted power, P_r is the received power, G_t is the transmit antenna gain, and G_r is the receive antenna gain. An ideal free space (FS) path (no ground reflection, no multipath, no signal attenuation) has a path loss which is proportional to the square ($n = 2$) of the separation D

$$L_{FS}(d) = 10n \log_{10}\left(\frac{4\pi D}{\lambda}\right)\bigg|_{n=2} \qquad (4.2)$$

where λ is the wavelength. This typically represents the minimum path loss and serves as a lower limit. Path loss exponents n on the order of 4 are more representative of the cluttered environments and low transmit antenna heights found at cellular base stations in built-up areas and areas obscured by terrain and vegetation.

4.1 Path Loss Data and Discussion

The basic transmission loss (L_{BT}) versus distance is plotted for the three frequencies (440 MHz, 1360 MHz, and 1920 MHz) and two transmitter locations in Figures 4.1 and 4.2. Each point in these scatter plots represents an average over a burst (128 impulses per burst, all impulses within a burst have the same GPS location tag). The data are then fit with a curve of the form

$$\overline{L_{BT}} = 10n \log_{10}(BD),$$ (4.3)

where B = distance multiplier
D= Distance in km.

This curve is linear with a slope of *n* when plotted on a log scale. Free space path loss (L_{FS}) is also plotted for the same three frequencies. The free-space curves serve as a "minimum" loss reference.

One loss parameter of interest is the ratio of the measured basic transmission loss to the free space loss at a given frequency, designated $\Delta L_{BT/FS}$. This parameter gives an indication of the additional loss due to scattering and diffraction within the channel. Also of interest is the ratio of the measured loss at 1360 MHz and 1920 MHz to the measured loss at 440 MHz, designated $\Delta L_{BT/440}$. This parameter gives an indication of the additional power needed at these higher frequencies when compared to the existing 440 MHz systems. These two parameters are highlighted in the discussion that follows and in Tables 3 to 6.

Figure 4.1 shows the L_{BT} data measured using the Anderson Mountain transmitter site. From the curve fit data we see that the path loss exponents, *n*, for the 440, 1360 and 1920 MHz frequencies are 3.3, 3.5 and 3.1 respectively. The 1360 MHz path loss exponent is from the van roof mounted antenna. L_{BT} is larger than the free space values at all distances, and this difference increases as distance increases. For example, at 2.0 km, the 440 MHz, 1360 MHz and 1920 MHz $L_{BT/FS}$ values are 15.6 dB, 15.8 dB and 16.4 dB respectively. This means that the path loss at these frequencies and distance is about 16 dB larger than predicted from the free space loss equation. At 20 km, $L_{BT/FS}$ is 28.7 dB, 31.3 dB and 27.3 dB respectively. The loss ratio for 1360 and 1920 MHz to the loss at 440 MHz ($\Delta L_{BT/440}$) is 10.1 dB and 13.7 dB at 2 km and 12.4 dB and 11.4 dB at 20 km respectively. This means that the best-fit ratio of measured loss at higher frequencies is 10 to 12 dB greater than the loss measured at 440 MHz using the Anderson Mountain transmitter site. These data are summarized in Table 3.

The path loss exponents for Pidcoke are 3.4, 3.9 and 3.1 for the 440, 1360 and 1920 MHz carrier frequencies. These data have only a slight increase in path loss exponents when compared to the Anderson Mountain site. However, the loss differential over free space increased using the lower transmitter at Pidcoke. At 1.0 km, $L_{BT/FS}$ values for 440 MHz, 1360 MHz and 1920 MHz are 22.2 dB, 19.5 dB and 24.2, all larger than the corresponding $L_{BT/FS}$ at 2.0 km for the Anderson Mountain site. At 10.0 km, $L_{BT/FS}$ values

6

for 440 MHz, 1360 MHz and 1920 MHz are 36.2 dB, 38.6 dB and 34.8, again all substantially larger than the corresponding $L_{BT/FS}$ values at 20.0 km for the Anderson Mountain site. However, the ratio of loss at 1360 and 1920 MHz to the loss at 440 MHz ($\Delta L_{BT/440}$) for Pidcoke is 7.1 and 14.8 dB at 1 km and 12.2 and 11.4 dB at 10 km. So moving to higher frequencies has a similar penalty for both transmitter sites. These values can be linearly interpolated for other distances in the measured range by multiplying the ratio of the distances in km by the slope. These data for Pidcoke are summarized in Table 4.

Table 3. Basic Transmission Loss, L_{BT}, Data for Anderson Mountain (Site 1)

| F (MHz) | L_{BT} Linear Fit Parameters | | Distance (km) | | | | | |
| | | | 2.0 | | | 20 | | |
	n	B (km^{-1})	L_{FS} (dB)	$\Delta L_{BT/FS}$ (dB)	$\Delta L_{BT/440}$ (dB)	L_{FS} (dB)	$\Delta L_{BT/FS}$ (dB)	$\Delta L_{BT/440}$ (dB)
440	3.3	848	91.3	15.6	N/A	111.3	28.7	N/A
1360	3.5	1010	101.1	15.8	10.1	121.1	31.3	12.4
1920	3.1	4107	104.1	16.4	13.7	124.1	27.3	11.4

Table 4. Basic Transmission Loss, L_{BT}, Data For Pidcoke Transmitter (Site 2)

| F (MHz) | L_{BT} Linear Fit Parameters | | Distance | | | | | |
| | | | 1.0 (km) | | | 10.0 (km) | | |
	n	B (km^{-1})	L_{FS} (dB)	$\Delta L_{BT/FS}$ (dB)	$\Delta L_{BT/440}$ (dB)	L_{FS} (dB)	$\Delta L_{BT/FS}$ (dB)	$\Delta L_{BT/440}$ (dB)
440	3.4	1451	85.3	22.2	N/A	105.3	36.2	N/A
1360	3.9	854	95.1	19.5	7.1	115.1	38.6	12.2
1920	3.1	9932	104.1	24.2	14.8	118.1	34.8	11.4

An alternative to curve fitting the measured data is to bin the L_{BT} data according to distance and compute the mean, standard deviation, and the 90% and 99% probability levels (i.e. 99% of the L_{BT} data in the bin are less than this level). These data give the upper bounds for the measured transmission loss, L_{BT}, and indicate transmit power levels needed to ensure a certain channel availability probability. The data are plotted in Figures 4.3 through 4.10 and summarized in Tables 5 and 6. Note that in these plots the data are not averaged over a burst as in Figures 4.1 and 4.2. The 99% L_{BT} levels range from 98.8 to 168 dB for the Anderson Mt. transmitter site and from 105.6 to 168 dB for the Pidcoke transmitter site. The 168 dB level represents the noise floor for the present system configuration. This limit is not reached for 440 MHz. However, at 1360 MHz and 1920 MHz, this limit is reached at approximately 11 km for Anderson Mt. and 7 km for Pidcoke.

Table 5. Anderson Mt. Basic Transmission Loss (L$_{BT}$), Free Space Loss (L$_{FS}$) and Measured Mean (Avg), 90%, and 99% Probability Levels

D (km)	L$_{FS}$ (dB)	L$_{BT}$ (dB): 440 MHz			L$_{FS}$ (dB)	L$_{BT}$ (dB): 1360 MHz (trailer)			L$_{FS}$ (dB)	L$_{BT}$ (dB): 1360 MHz (van)			L$_{FS}$ (dB)	L$_{BT}$ (dB): 1920 MHz		
		Avg	90%	99%		Avg	90%	99%		Avg	90%	99%		Avg	90%	99%
0.7	82.8	92.2	96.9	98.8	92.6	106.0	120.7	125.3	92.6	104.3	114.6	119.6	95.6	105.6	110.4	112.6
1.8	90.3	106.8	113.9	114.1	100.1	117.7	125.8	126.3	100.1	116.2	119.7	120.1	103.1	123.9	127.1	128.4
2.8	94.2	110.1	120.3	122.1	104.0	121.9	130.0	133.2	104.0	121.1	132.6	138.2	107.0	125.6	137.6	139.1
3.8	96.9	112.5	126.5	130.3	106.7	128.1	144.9	149.9	106.7	125.2	145.1	152.7	109.7	127.8	144.1	148.9
4.8	99.0	119.8	125.2	127.1	108.8	135.6	147.5	156.5	108.8	136.4	152.9	160.7	111.8	137.6	146.6	155.8
5.8	100.6	120.2	131.3	137.2	110.4	135.8	152.0	159.0	110.4	131.5	150.3	155.9	113.4	132.5	149.6	154.2
6.9	102.0	127.2	142.1	145.0	111.8	141.7	165.7	166.8	111.8	141.9	165.2	166.4	114.8	144.3	161.9	164.3
7.9	103.2	121.3	129.6	138.1	113.0	136.8	151.7	162.5	113.0	128.8	142.2	161.1	116.0	130.0	141.7	150.7
8.9	104.3	129.9	140.7	146.3	114.1	145.8	159.7	165.9	114.1	141.7	162.7	166.0	117.1	140.6	156.1	161.3
9.9	105.2	131.0	135.4	138.5	115.0	145.1	154.7	160.5	115.0	142.8	154.3	162.1	118.0	142.5	149.9	155.0
10.9	106.1	148.5	156.2	158.2	115.9	161.3	166.6	167.3	115.9	162.6	166.2	166.9	118.9	158.8	165.9	166.9
12.0	106.9	147.3	159.3	160.7	116.7	160.8	166.7	167.3	116.7	159.5	166.4	167.1	119.7	158.6	166.4	167.1
13.0	107.6	140.3	149.9	158.0	117.4	157.5	166.3	167.2	117.4	158.0	165.9	166.9	120.4	156.9	165.7	166.7
14.0	108.2	136.2	144.5	151.1	118.0	151.8	164.5	166.7	118.0	151.7	165.2	166.3	121.0	147.9	159.0	164.1
15.0	108.8	134.8	157.3	159.3	118.6	154.1	166.6	167.5	118.6	142.7	166.4	167.2	121.6	144.0	166.2	167.1
16.0	109.4	129.2	145.2	158.6	119.2	141.0	161.5	166.7	119.2	140.0	164.9	166.5	122.2	140.6	160.6	166.5
17.1	110.0	132.6	151.3	153.9	119.8	154.7	166.0	167.1	119.8	149.6	165.8	166.8	122.7	147.2	165.5	166.7
18.1	110.5	131.5	144.8	151.4	120.3	149.0	165.8	167.1	120.3	147.7	165.6	166.6	123.3	146.3	163.4	165.9
19.1	110.9	142.4	150.8	152.8	120.7	160.3	166.7	167.3	120.7	157.6	166.3	167.0	123.7	154.7	166.3	166.9
20.1	111.4	145.2	158.5	160.2	121.2	159.4	166.7	167.5	121.2	159.9	166.3	167.0	124.2	157.9	166.3	167.0

Table 6. Pidcoke Basic Transmission Loss (L$_{BT}$), Free Space Loss (L$_{FS}$) and Measured Mean (Avg), 90%, and 99% Probability Levels

D (km)	L$_{FS}$ (dB)	L$_{BT}$ (dB): 440 MHz			L$_{FS}$ (dB)	L$_{BT}$ (dB): 1360 MHz (trailer)			L$_{FS}$ (dB)	L$_{BT}$ (dB): 1360 MHz (van)			L$_{FS}$ (dB)	L$_{BT}$ (dB): 1920 MHz		
		Avg	90%	99%		Avg	90%	99%		Avg	90%	99%		Avg	90%	99%
0.3	75.1	92.2	97.1	105.6	84.9	107.6	113.9	124.9	84.9	108.1	116.7	125.1	87.9	109.2	120.5	126.5
0.7	81.7	107.4	114.0	119.4	91.5	121.8	127.9	130.0	91.5	111.2	122.0	126.6	94.5	115.1	129.8	134.4
1.0	85.4	106.3	114.6	116.2	95.2	122.6	127.2	128.7	95.2	114.5	124.4	126.3	98.2	118.2	128.1	130.6
1.4	87.9	111.4	114.3	115.1	97.7	129.5	134.9	138.8	97.7	116.1	119.6	126.7	100.7	120.9	129.0	136.8
2.0	91.5	130.3	143.4	150.8	101.3	153.4	166.4	167.4	101.3	148.6	165.4	166.5	104.3	150.4	165.9	166.9
3.1	95.1	113.7	124.4	128.4	104.9	138.4	144.8	151.2	104.9	128.4	142.7	146.2	107.9	130.6	141.0	146.7
4.1	97.6	130.2	149.9	155.4	107.4	145.5	158.7	164.6	107.4	143.7	164.0	165.9	110.4	141.8	156.0	161.2
5.2	99.6	122.4	128.8	135.4	109.4	140.3	155.1	160.3	109.4	133.6	145.2	154.9	112.4	133.6	142.9	154.1
6.2	101.2	131.8	140.4	143.4	111.0	146.7	157.8	165.2	111.0	144.1	159.9	166.2	114.0	143.0	155.2	163.8
7.3	102.5	131.4	151.1	155.4	112.3	141.5	165.7	167.2	112.3	139.6	166.0	166.9	115.3	142.4	165.3	166.9
8.0	103.3	133.7	144.2	146.8	113.1	147.6	164.6	167.1	113.1	147.9	165.5	166.6	116.1	146.0	160.4	166.2
9.0	104.4	139.6	155.2	157.0	114.2	158.1	166.9	167.7	114.2	158.2	166.2	166.9	117.2	153.8	166.3	167.2
10.1	105.4	152.5	157.5	158.9	115.2	165.0	167.5	168.1	115.2	164.8	166.6	167.2	118.2	164.1	167.1	167.7
11.1	106.2	150.8	156.5	158.1	116.0	164.5	167.3	167.9	116.0	164.9	166.5	167.1	119.0	162.7	166.9	167.7
12.1	107.0	140.9	148.1	151.3	116.8	159.8	166.4	167.5	116.8	157.4	166.0	166.9	119.8	150.3	165.0	167.2
13.2	107.7	146.5	156.8	158.8	117.5	159.2	167.2	168.2	117.5	161.4	166.5	167.1	120.5	157.0	166.7	167.5
13.9	108.2	142.9	151.4	156.3	118.0	157.4	166.0	167.5	118.0	160.8	165.8	167.0	121.0	154.0	164.5	166.7

The L$_{BT}$ data can also be plotted on maps as in Figures 4.11 through 4.18. These maps show the spatial distribution of L$_{BT}$ along the various cell-route combinations. They are useful for anticipating areas where there will be coverage problems from a given transmitter site.

The effects of receiver antenna height were studied by adding an additional 1360 MHz channel and placing its antenna on a low trailer behind the measurement van. Data for this channel are compared to data from a "high" antenna mounted on the van roof. Figures 4.19 and 4.20 are scatterplots of L$_{BT}$, comparing these two antennas for each transmitter site. Using the curve fit data for Anderson Mountain, we see that the low antenna has a similar path loss exponent but about 2 to 3 dB more basic transmission loss. For Pidcoke the basic transmission loss differential is hard to estimate because the

path loss exponents or slopes of the curves were different, causing the curves to intersect near 10 km.

5. DELAY STATISTICS

The delay statistics presented in this report are based on averaged power delay profiles (APDPs)

$$APDP(t_i) = \frac{1}{N} \sum_{k=1}^{N} PDP_k(t_i) \quad , \tag{5.1}$$

where t_i is the i-th time step (sampling point), and N is the number of PDPs used to form the APDP. The PDP is the magnitude squared (power) of the measured impulse response. The use of averaging significantly reduces the contribution of noise to the delay statistics. The ATB burst configuration software was set to produce 128 impulses per burst for these measurements. APDPs were calculated from groups of 8 successive PDPs. Thus, each burst yields 16 APDPs (128/8). The choice of 8 as the group size makes efficient use of all the burst data. APDPs were computed separately for each channel.

Impulses within an APDP group (8 successive PDPs) were first checked for sufficient power. The impulse with the maximum total signal power was found by integration over the full time interval. Impulses with total signal power more than 10 dB below this group maximum were discarded for the APDP statistics. Groups containing less than 4 usable PDP's are discarded as well. Thus, N ranges from 4 to 8 in (5.1) above.

Referring to Figure 5.1, the interval of discrimination (ID) is here defined as the difference in power levels between the peak of the intended signal (impulse) and the peak noise. It is desired that an APDP have an ID sufficient to ensure that noise does not contaminate the fading statistics. For the data here, 23 dB and 13 dB ID criteria have been used. The 23 dB margin gives the maximum useful dynamic range for analog applications, while the 13 dB threshold may be more useful for digital applications. If the ID is less than 23 dB or 13 dB respectively, then the APDP was discarded for that data set. For valid APDPs, signal levels within 20 dB and 10 dB respectively of the APDP peak were included in the delay statistics, as indicated in Figure 5.1. This corrected APDP ensures that noise is not included. We expect the 20 dB criterion to yield longer delays but fewer valid APDPs than will the 10 dB criterion.

Three delay measures were considered: maximum delay, mean delay, and RMS delay spread. The maximum delay was defined as the time delay between the first and last signals of that portion of the corrected APDP (see Fig. 5.1). The mean delay (*d*) was the time-weighted average, or first moment, of the corrected APDPs normalized by the average signal power,

$$mean\ delay = d = \frac{\frac{1}{N}\sum\limits_{k=1}^{N} t_k P(t_k)}{\frac{1}{N}\sum\limits_{k=1}^{N} P(t_k)} = \frac{\sum\limits_{k=1}^{N} t_k P(t_k)}{\sum\limits_{k=1}^{N} P(t_k)} \qquad , \qquad (5.2)$$

where t_k is the time delay (in seconds) relative to the start of the corrected APDP (i.e. $t = 0$), P is the signal power (W), and N is the index of the final corrected APDP signal point considered. The RMS delay spread (S) measures the standard deviation of the delay spread of each corrected APDP about its mean delay (d). It is the second central moment of the corrected APDP given by

$$RMS\ delay\ spread = S = \left[\frac{\sum\limits_{k=1}^{N}(t_k - d)^2 P(t_k)}{\sum\limits_{k=1}^{N} P(t_k)}\right]^{1/2} . \qquad (5.3)$$

Figures 5.2 through 5.7 show the cumulative probability distributions (CDFs) for the two transmitter sites (Anderson Mt. and Pidcoke) using 23 dB ID and 20 dB corrected APDP levels. Figures 5.8 through 5.13 show the corresponding data for the 13 dB ID and 10 dB corrected APDP levels. The CDF data are summarized in Tables 7 through 10 which give the maximum delay (max), mean delay (avg), and RMS delay spread (spr) in microseconds observed at the 90%, 99%, and 99.9% probability levels. Also included in the tables are the percentages of valid APDPs for each of the transmitter, ID, and frequency combinations.

Figures 5.14 through 5.21 show the RMS Delay Spread data on site maps. Gaps indicate areas where the signal strength was too low to calculate delay spread. Using these maps, specific areas with multipath can be identified. In general they show that most areas had small delay spreads near the resolution limit of the measurment system, which is between 20 and 30 ns using a 20 dB ID.

Table 7. Anderson Mt.: Delay Statistics for APDPs with a 20 dB ID

	440 MHz			1360 MHz (Trailer)			1360 MHz (Van)			1920 MHz		
	69 % APDPs Valid			52 % APDPs Valid			52 % APDPs Valid			61 % APDPs Valid		
Prob.	Delay (µs)			Delay (µs)			Delay (µs)			Delay (µs)		
(%)	max	Avg	spr	max	avg	spr	max	avg	spr	max	avg	spr
90.0	0.93	0.15	0.15	0.75	0.15	0.13	0.55	0.13	0.08	0.65	0.13	0.09
99.0	17.4	1.52	3.92	12.1	1.26	2.59	14.7	1.57	3.48	12.0	1.78	3.35
99.9	23.1	17.8	7.03	39.3	22.1	9.21	20.8	17.4	6.06	24.3	18.4	8.30

Table 8. Anderson Mt.: Delay Statistics for APDPs with a 10 dB ID

Prob. (%)	440 MHz			1360 MHz (Trailer)			1360 MHz (Van)			1920 MHz		
	81 % APDPs Valid			69 % APDPs Valid			67 % APDPs Valid			74 % APDPs Valid		
	Delay (μs)			Delay (μs)			Delay (μs)			Delay (μs)		
	max	Avg	spr	max	avg	spr	max	avg	spr	max	avg	spr
90.0	0.13	0.09	0.03	0.23	0.11	0.06	0.15	0.09	0.03	0.15	0.09	0.04
99.0	1.65	0.30	0.46	9.43	3.25	3.03	2.33	0.72	0.74	7.15	3.71	3.08
99.9	7.13	1.84	2.30	23.7	10.5	8.59	10.9	7.02	3.55	23.7	8.69	9.15

Table 9. Pidcoke: Delay Statistics for APDPs with a 20 dB ID

Prob. (%)	440 MHz			1360 MHz (Trailer)			1360 MHz (Van)			1920 MHz		
	60 % APDPs Valid			43 % APDPs Valid			42 % APDPs Valid			56 % APDPs Valid		
	Delay (μs)			Delay (μs)			Delay (μs)			Delay (μs)		
	max	avg	spr	max	avg	spr	max	avg	spr	max	avg	spr
90.0	0.93	0.16	0.14	0.75	0.16	0.12	0.56	0.14	0.09	1.18	0.18	0.19
99.0	9.70	1.14	2.26	10.2	1.94	2.59	3.48	0.40	0.77	7.25	0.93	1.67
99.9	17.5	3.89	5.40	19.0	3.21	5.39	18.9	1.32	3.78	10.9	2.56	2.77

Table 10. Pidcoke: Delay Statistics for APDPs with a 10 dB ID

Prob. (%)	440 MHz			1360 MHz (Trailer)			1360 MHz (Van)			1920 MHz		
	76 % APDPs Valid			60 % APDPs Valid			59 % APDPs Valid			69 % APDPs Valid		
	Delay (μs)			Delay (μs)			Delay (μs)			Delay (μs)		
	max	avg	spr	max	avg	spr	max	avg	spr	max	avg	spr
90.0	0.13	0.09	0.03	0.30	0.13	0.07	0.18	0.10	0.04	0.18	0.10	0.04
99.0	2.10	0.75	0.88	5.88	2.73	2.21	2.18	0.64	0.72	3.48	0.88	1.17
99.9	9.73	2.93	3.69	14.5	5.49	4.97	7.58	1.96	2.59	13.5	5.52	4.69

6. REFERENCES

[1]   J. A. Wepman, J. R. Hoffman, L. Loew and V. S. Lawrence, "Comparison of wideband propagation in the 902-928 and 1850-1990 MHz bands in various macrocellular environments," NTIA Report 93-299, Sep. 1993.

[2]   J. A. Wepman, J. R. Hoffman and L. Loew, "Impulse response measurements in the 1850-1990 MHz band in large outdoor cells", NTIA Report 94-309, June 1994.

[3]   P. Wilson, P. Papazian, M. Cotton and Y. Lo, "Advanced antenna test bed characterization for wideband wireless communication systems," NTIA Report 99-369, August 1999.

[4]   P. Papazian, K. Allen and M. Cotton, "A test bed for the evaluation of adaptive antennas used for mobile communications", in *Proc. IEEE Aerospace Conference*, Snowmass, CO, Mar. 1998, paper #161.

[5]   M. Weiner, S. Cruze, C. Li and W. Wilson, Ch. 3 of *Monopole Elements on Circular Ground Planes*, Norwood, MA: Artech House, 1987, pp. 19-76.

7. FIGURES

Figure 2.1. Anderson Mountain transmitter site showing mast and antenna mount.

Figure 2.2. View looking north from Anderson Mountain.

Figure 2.3. Van with trailer at Pidcoke transmitter site.

Figure 2.4. Measurement crew at Pidcoke transmitter site.
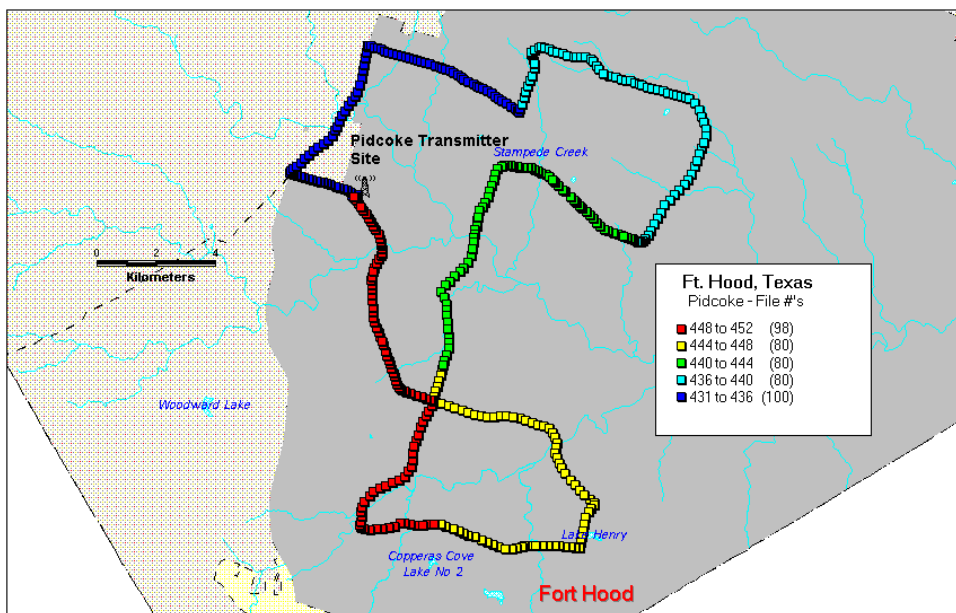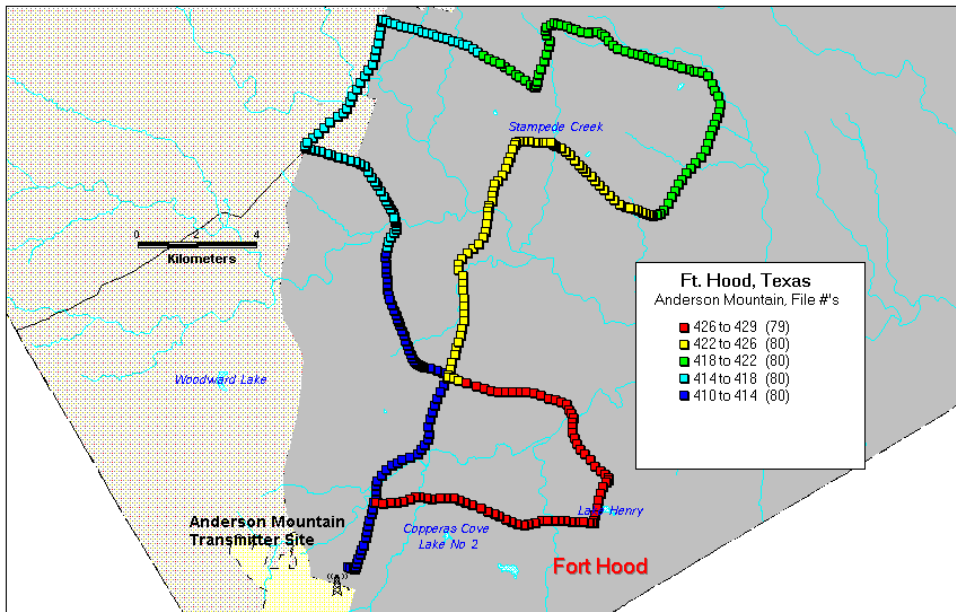
Figure 2.5. Anderson Mountain transmitter site and drive route, Ft. Hood, Texas.
Figure 2.6. Pidcoke transmitter site and drive route, Ft. Hood, Texas
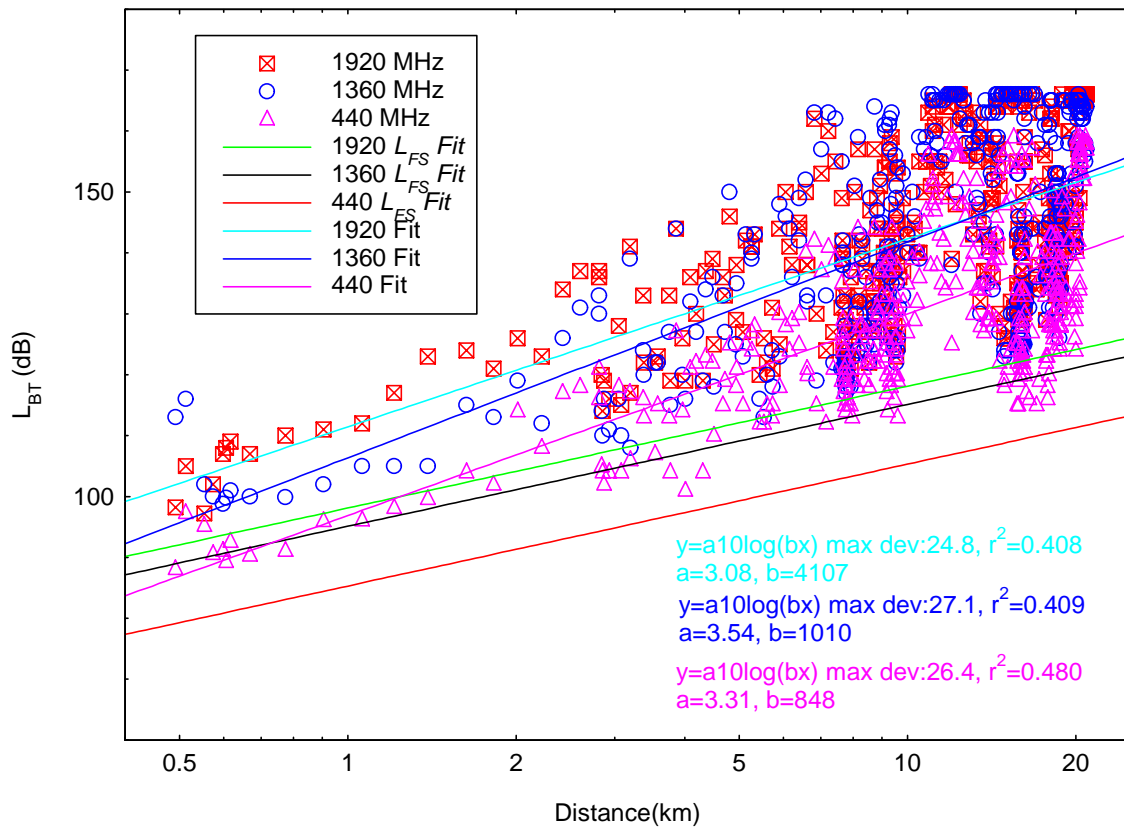
Figure 4.1 Basic transmission loss scatterplot, Anderson Mountain transmitter site.
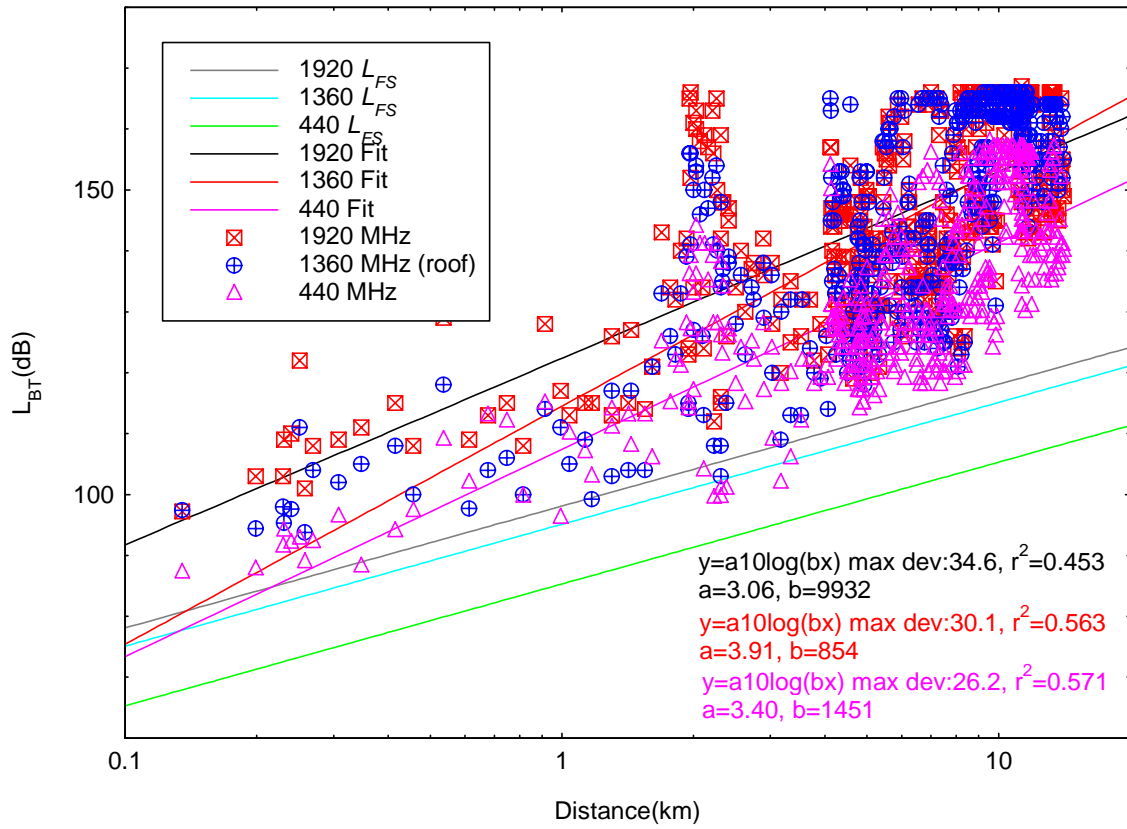
Figure 4.2 Basic transmission loss scatterplot, Pidcoke transmitter site.
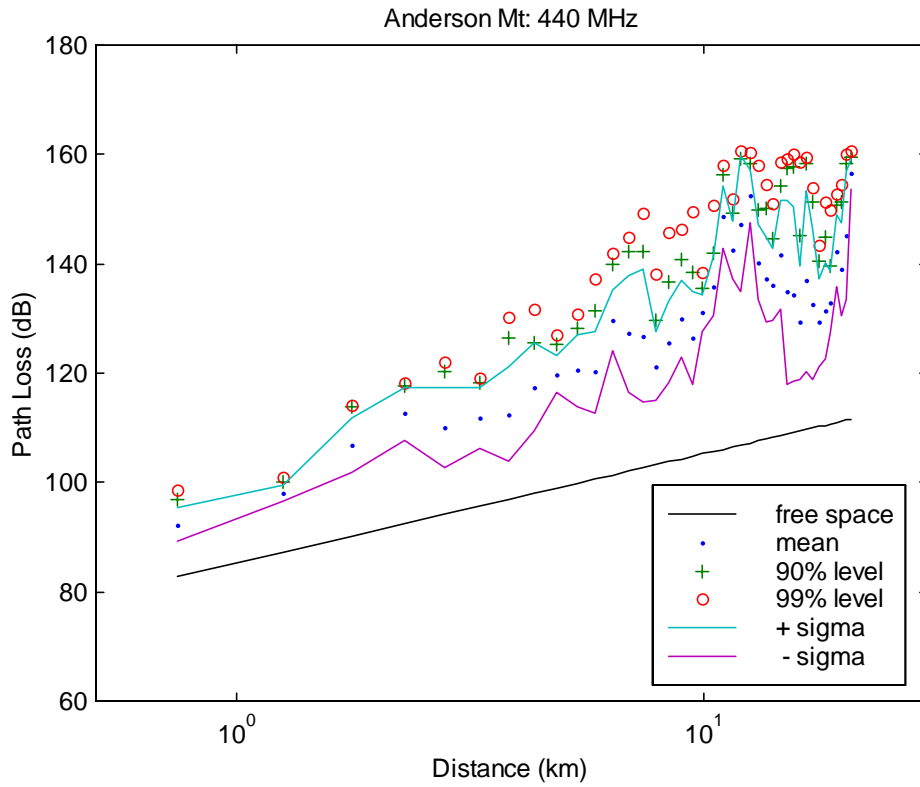
Figure 4.3. Basic transmision loss variance, Anderson Mt., 440 MHz.
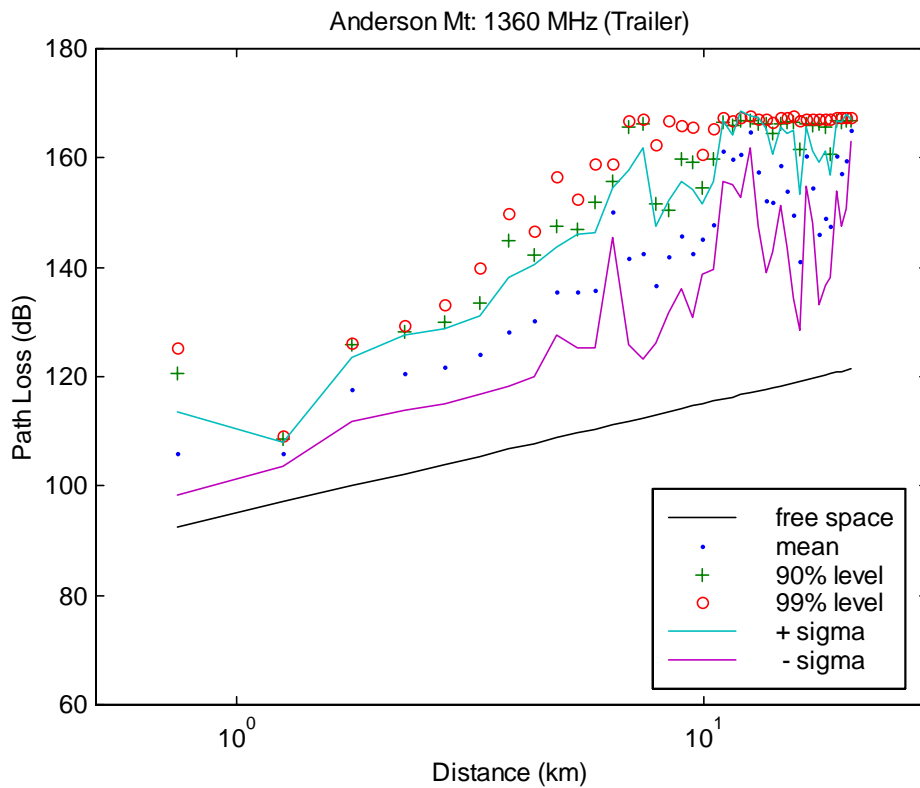
Figure 4.4. Basic transmision loss variance (trailer), Anderson Mt., 1360 MHz.
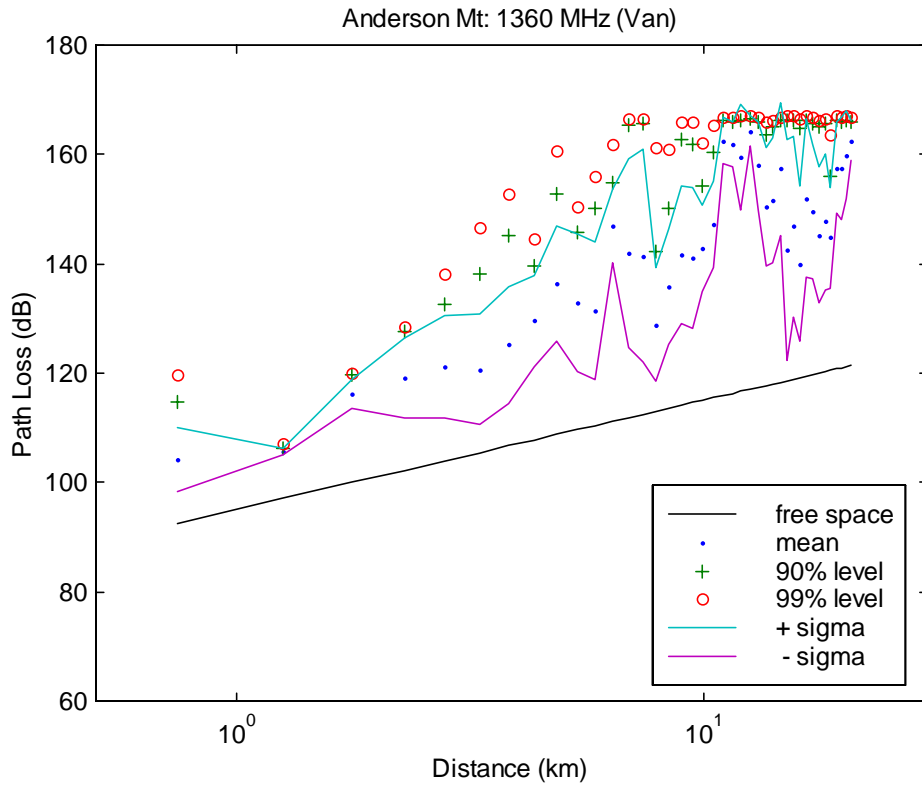
Figure 4.5. Basic transmision loss variance (van), Anderson Mt., 1360 MHz.
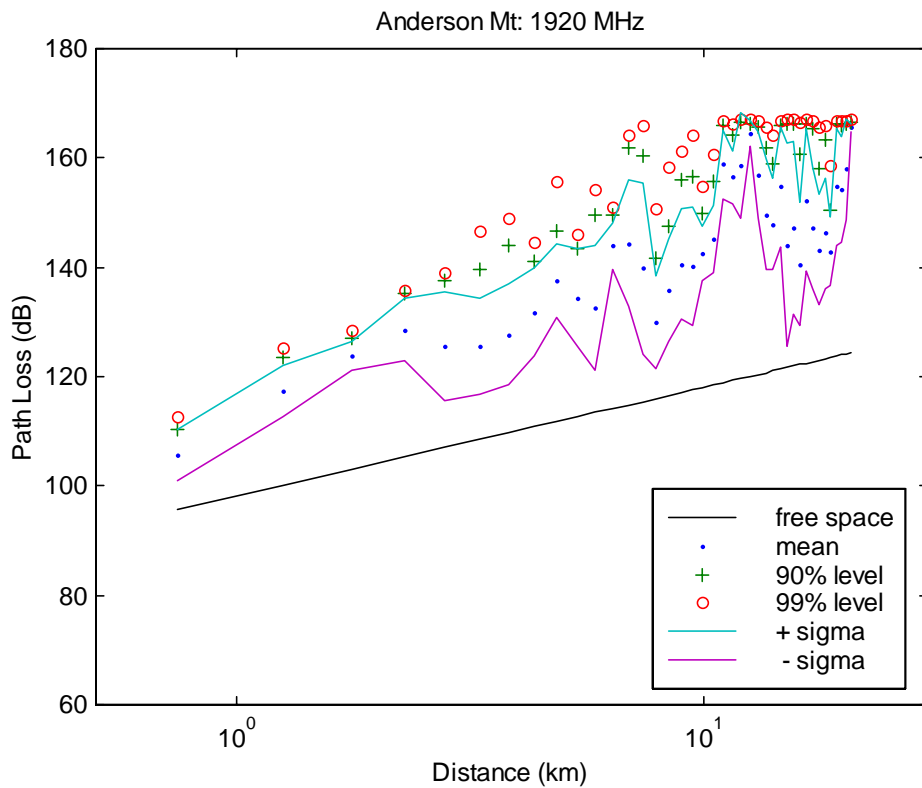
Figure 4.6. Basic transmision loss variance, Anderson Mt., 1920 MHz.
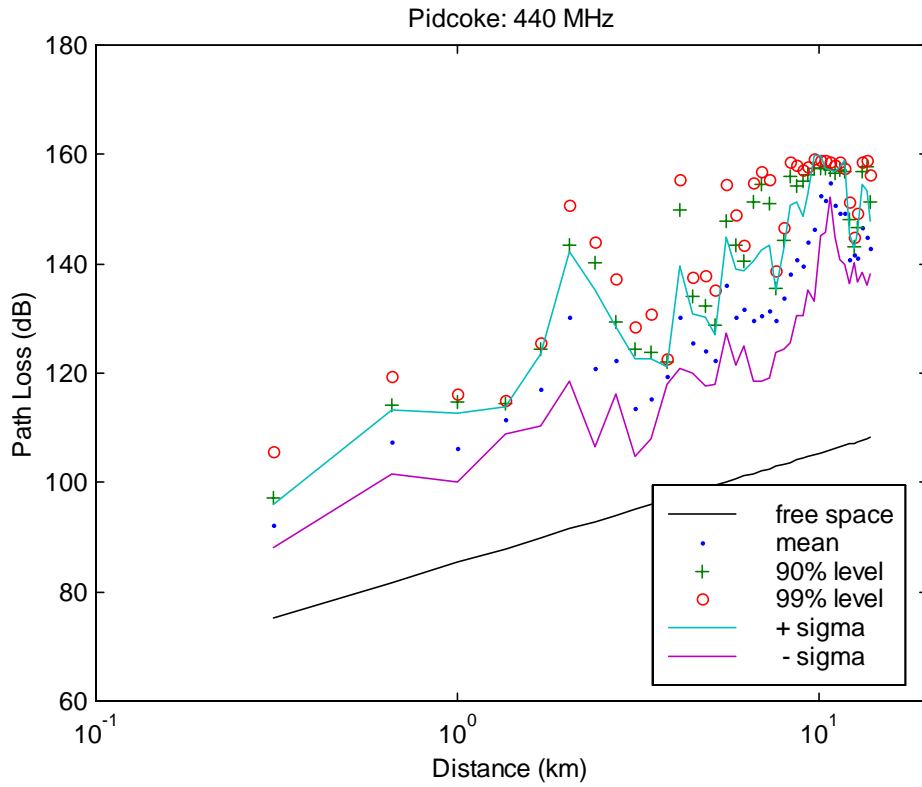
Figure 4.7. Basic transmision loss variance, Pidcoke, 440 MHz.
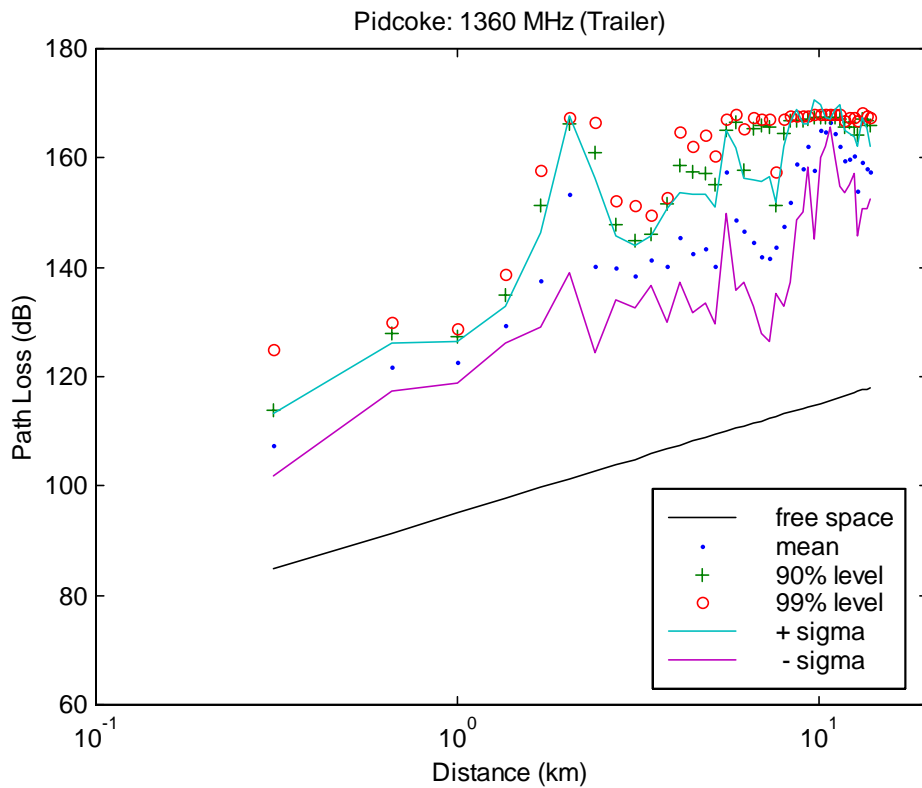
Figure 4.8. Basic transmision loss variance (trailer), Pidcoke, 1360 MHz.

Pidcoke: 1360 MHz (Van)
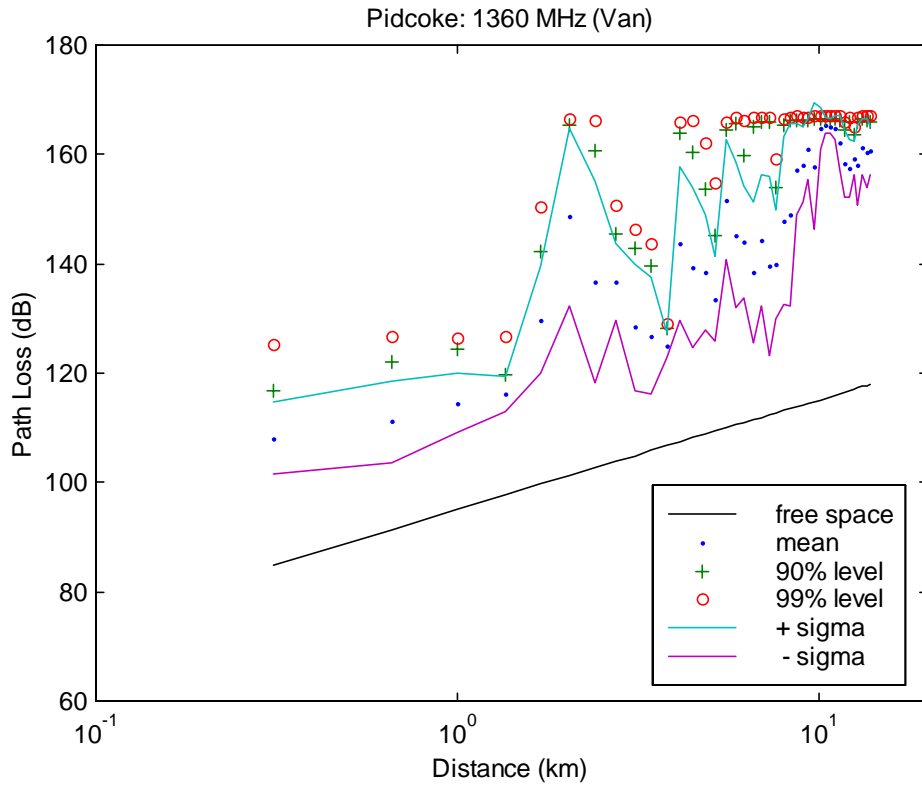
Figure 4.9. Basic transmision loss variance (van), Pidcoke, 1360 MHz.
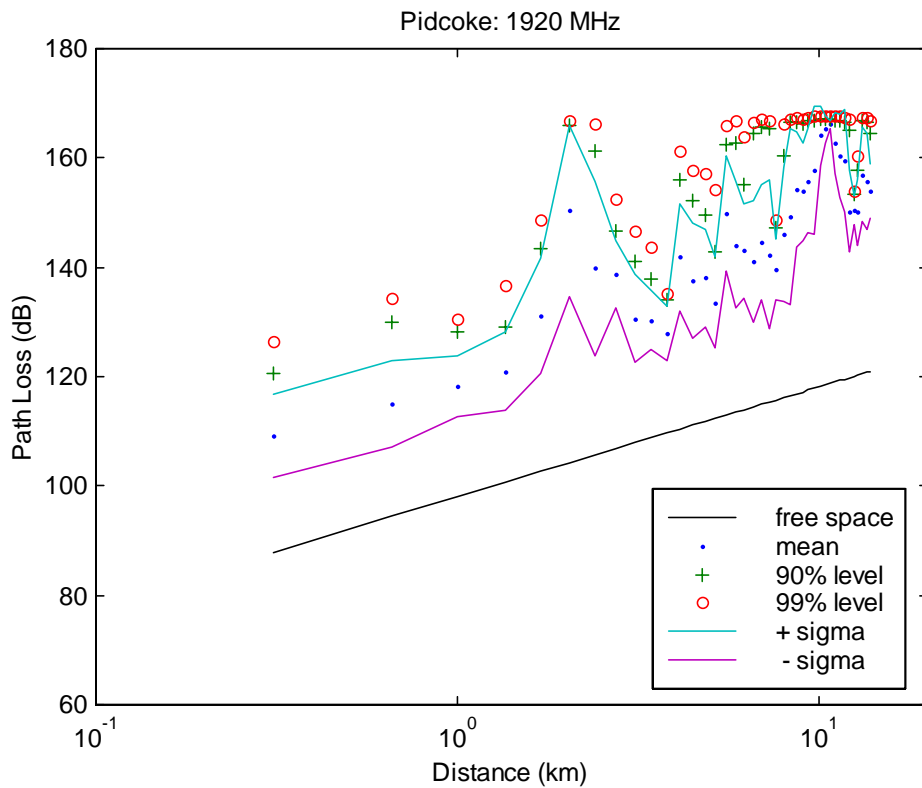
Pidcoke: 1920 MHz

Figure 4.10. Basic transmision loss variance, Pidcoke, 1920 MHz.
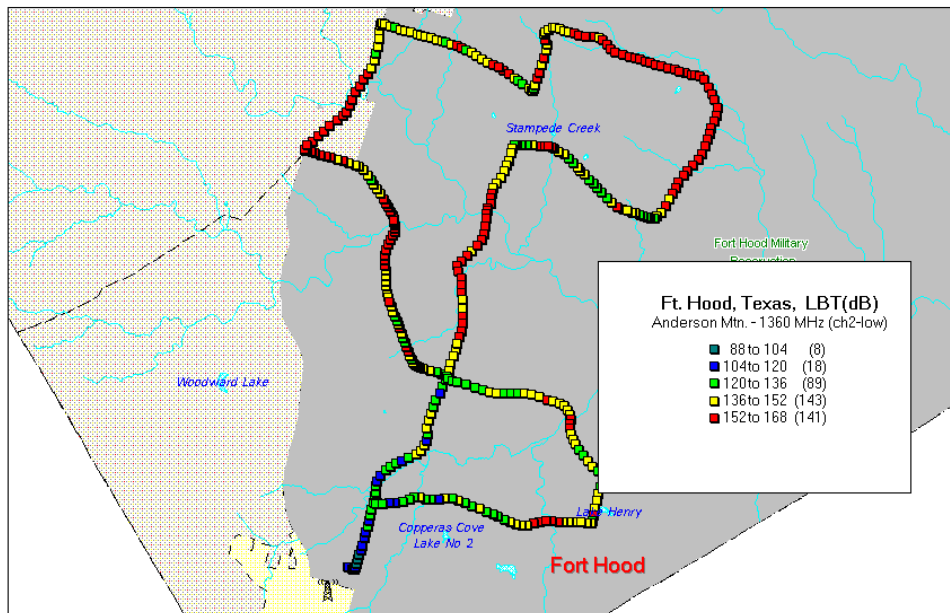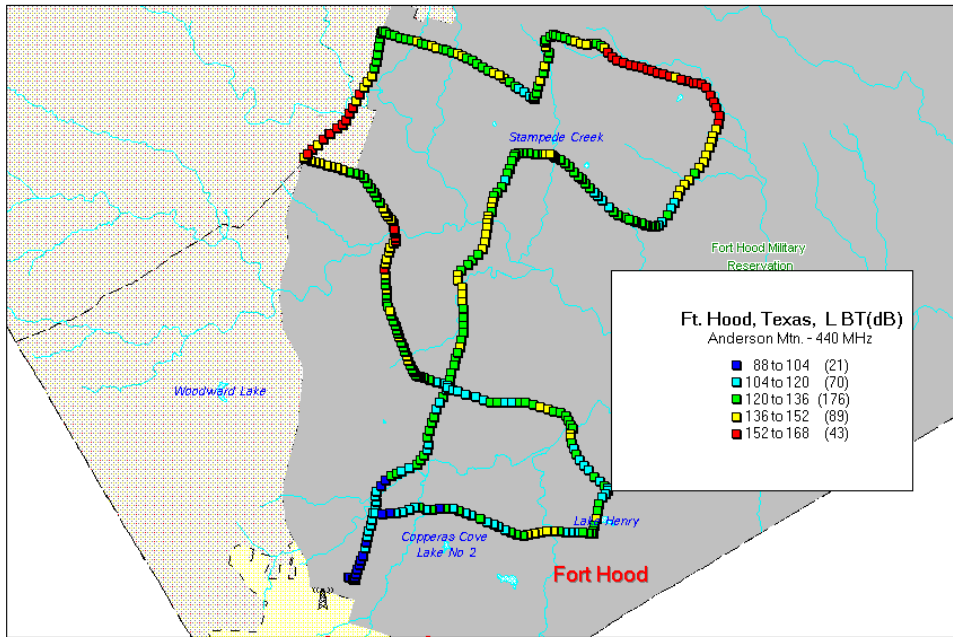
Figure 4.11. Basic transmission loss map, 440 MHz, Anderson Mountain.
Figure 4.12. Basic transmission loss map, 1360 MHz (low antenna), Anderson Mountain.
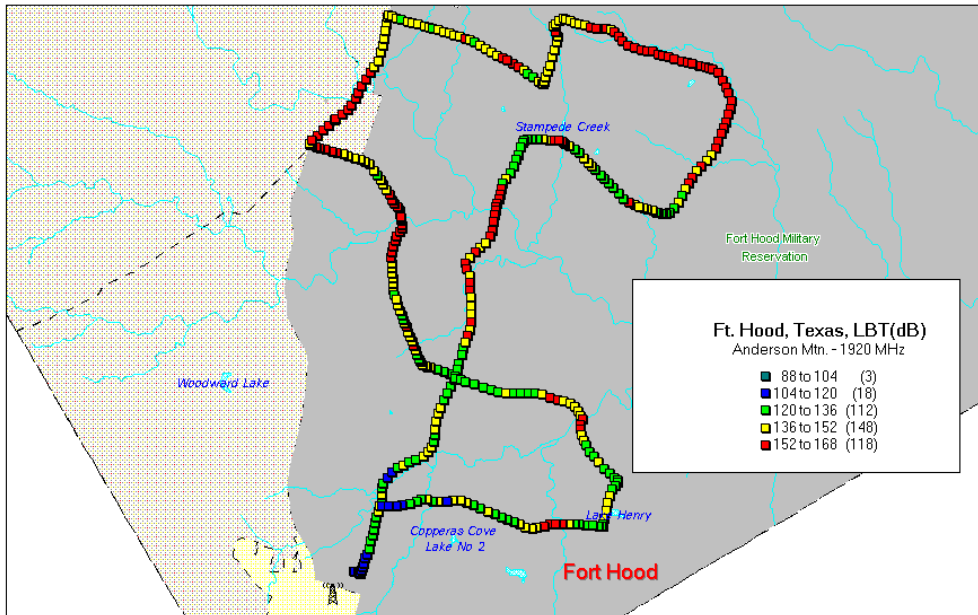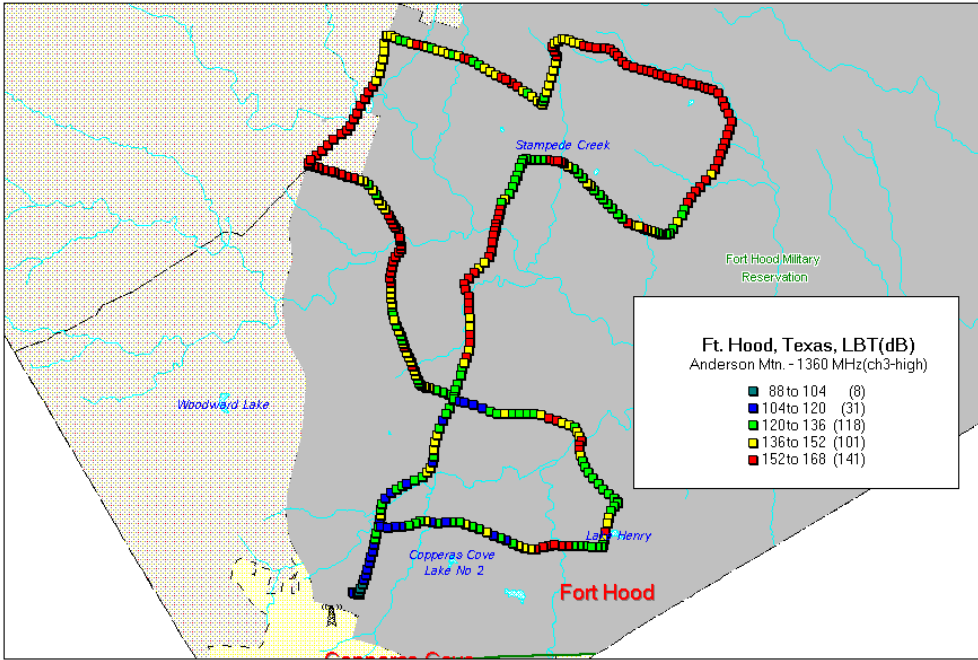
Figure 4.13 Basic transmission loss map, 1360 MHz (high antenna), Anderson Mountain.
Figure 4.14 Basic transmission loss map, 1920 MHz, Anderson Mountain.
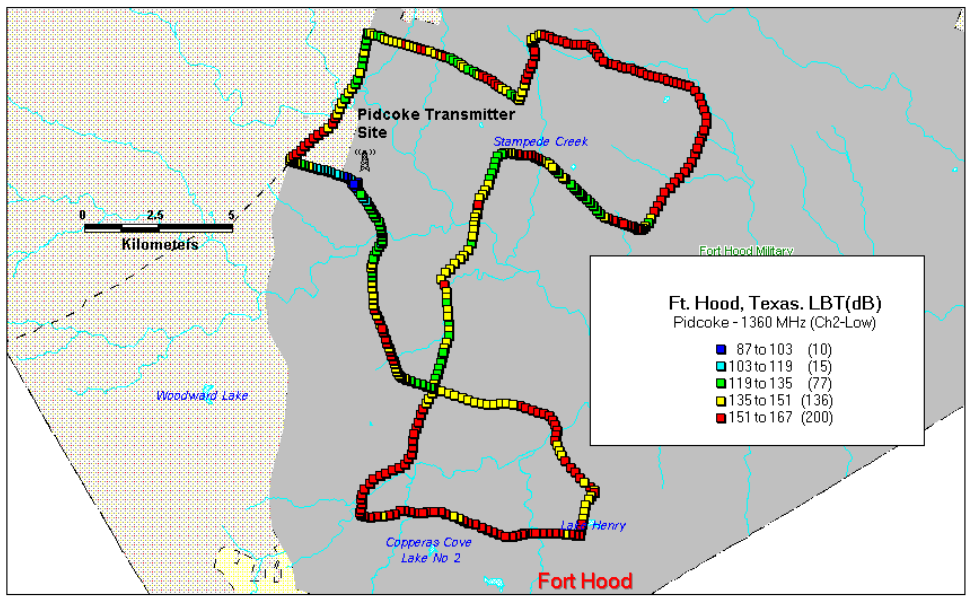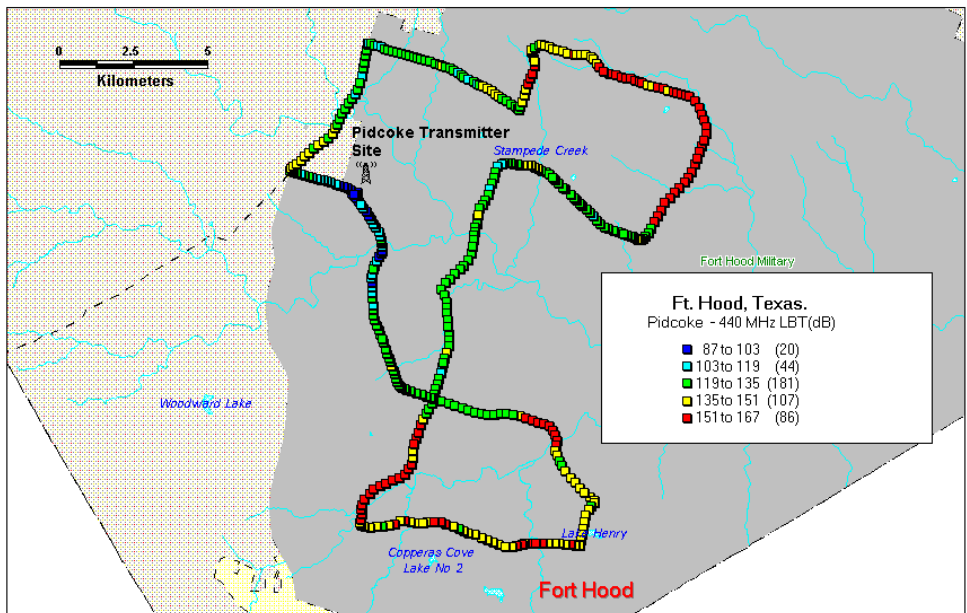
Figure 4.15. Basic transmission loss map, 440 MHz, Pidcoke.
Figure 4.16. Basic transmission loss map, 1360 MHz (low antenna), Pidcoke.
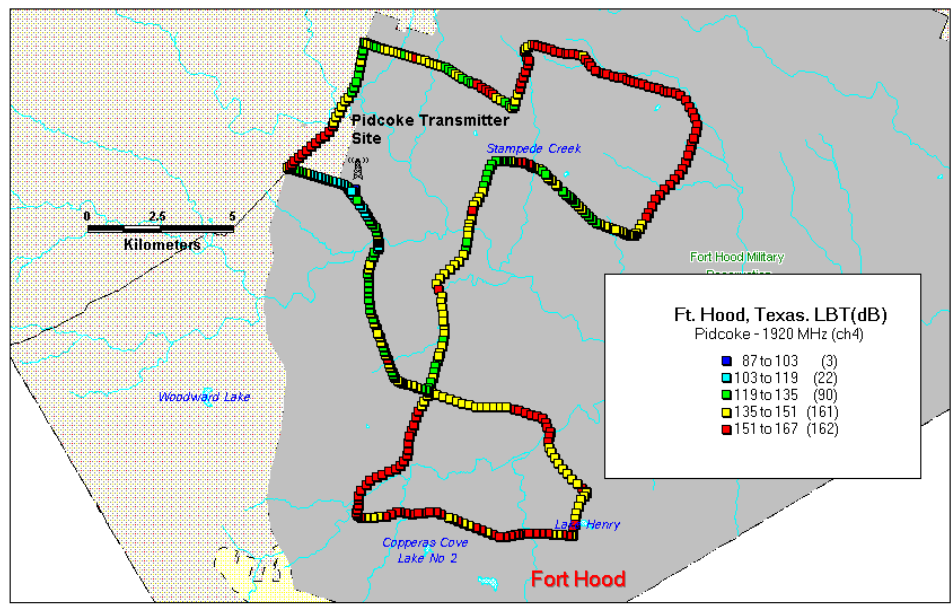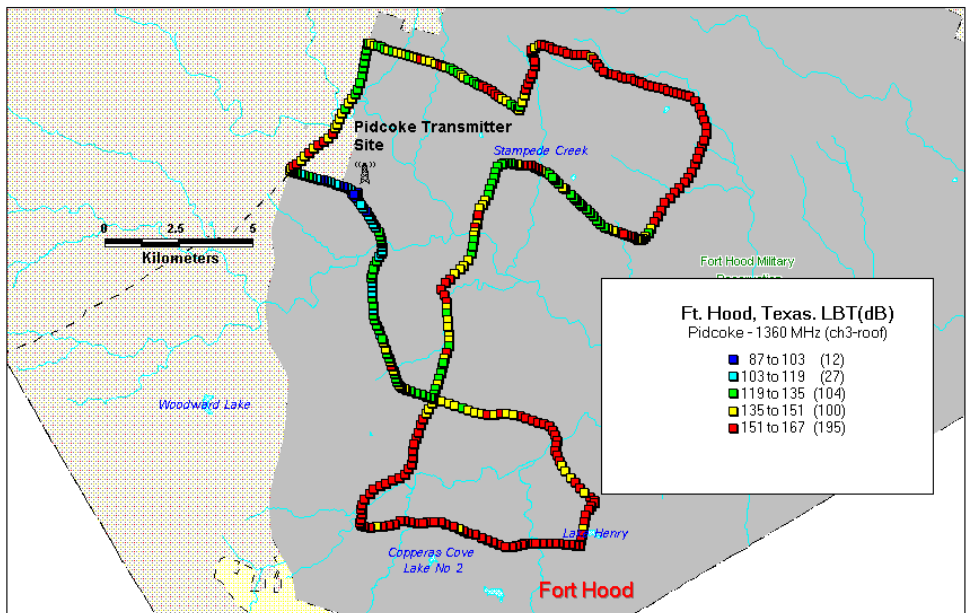
Figure 4.17. Basic transmission loss map, 1360 MHz (high antenna), Pidcoke.
Figure 4.18. Basic transmission loss map, 1920 MHz, Pidcoke.
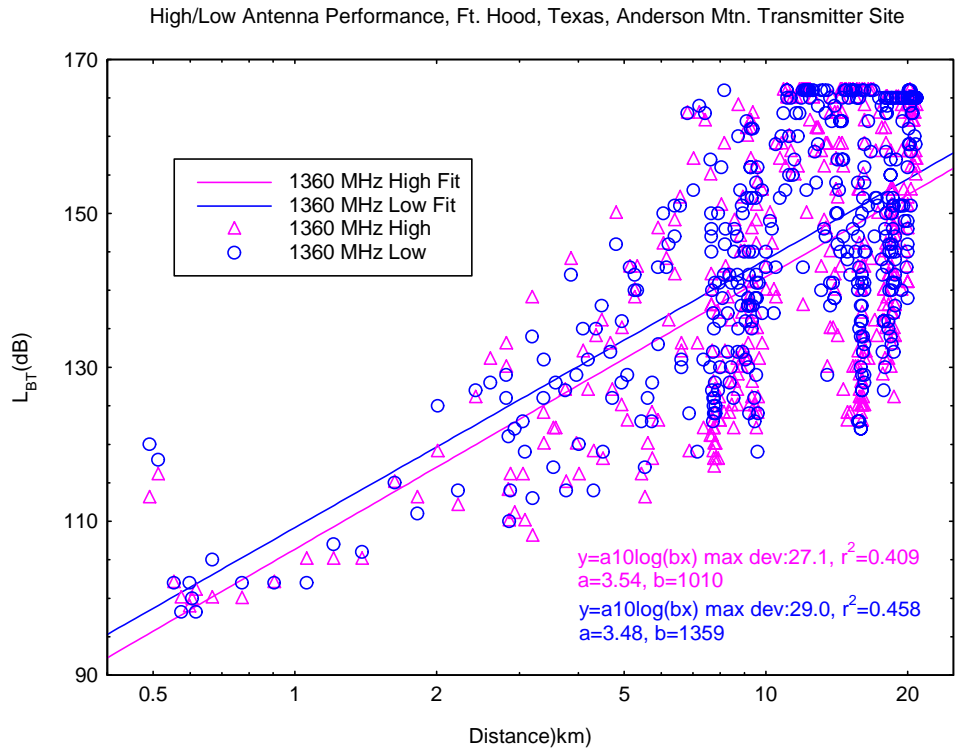
Figure 4.19. Basic transmission loss differential for low versus high 1360 MHz receive antennas from Anderson Mountain transmitter site.
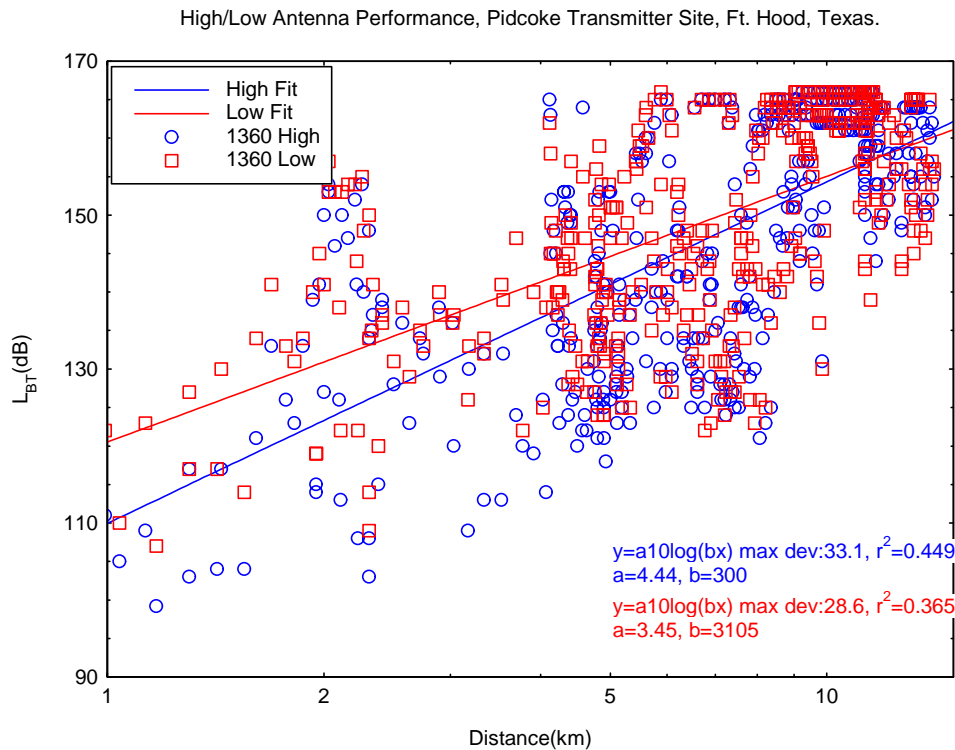
Figure 4.20. Basic transmission loss differential for low versus high 1360 MHz receive antennas from Pidcoke transmitter site.

27
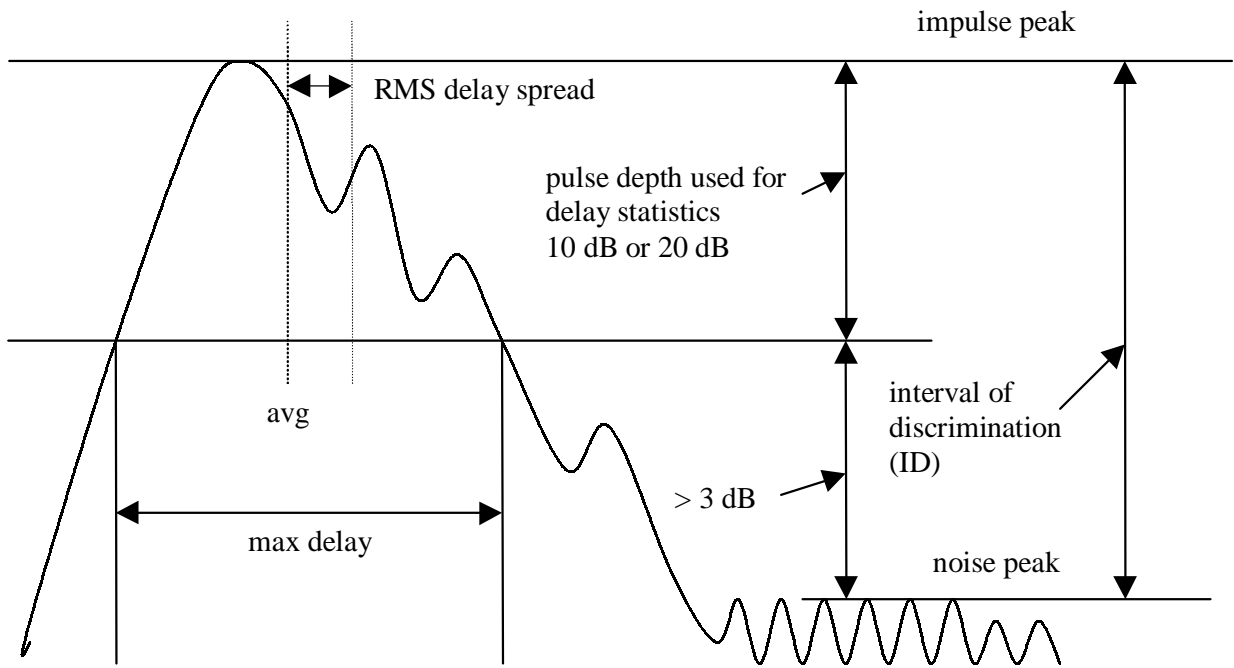
Figure 5.1. Idealized impulse response diagram with descriptive terminology.
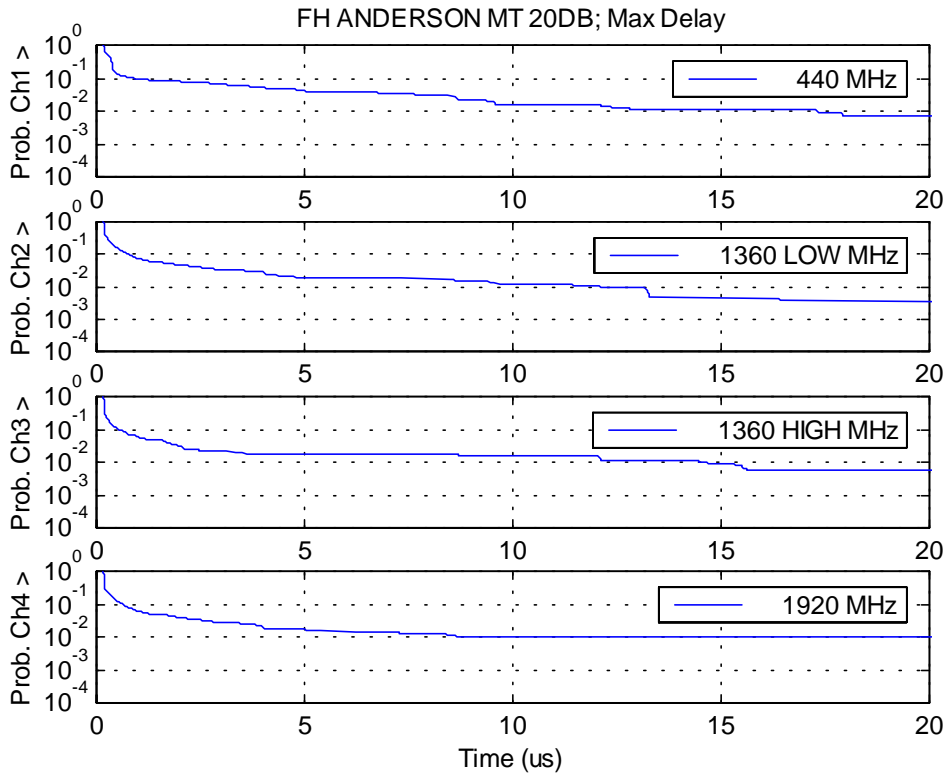
Figure 5.2. Anderson Mt. 20 dB ID: maximum delay CDF.
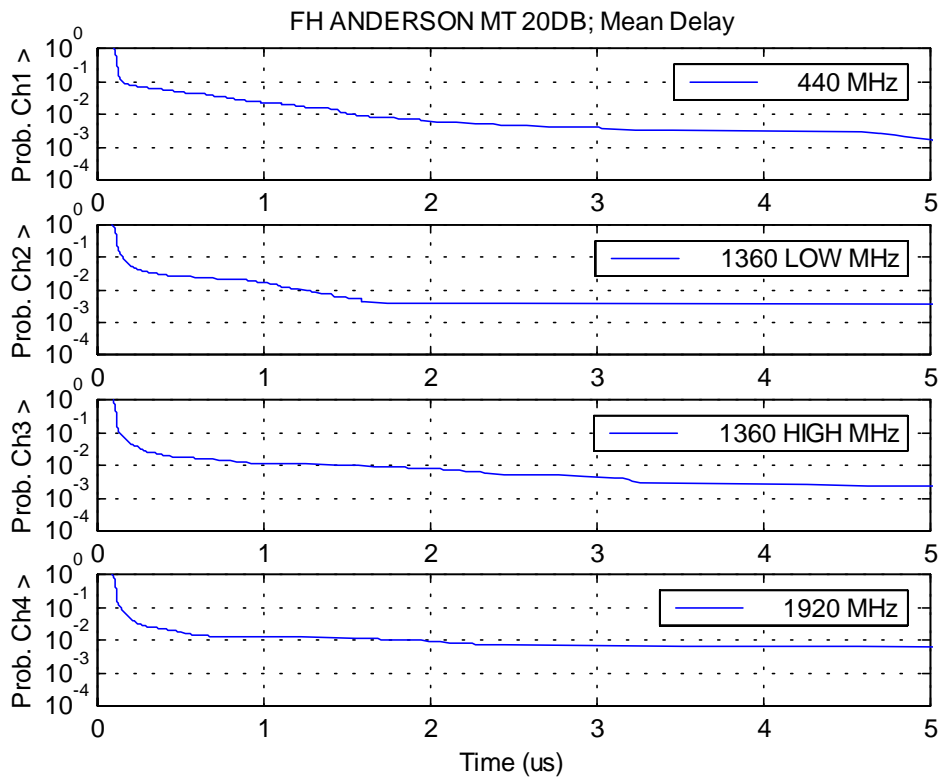
Figure 5.3. Anderson Mt. 20 dB ID: mean delay CDF.
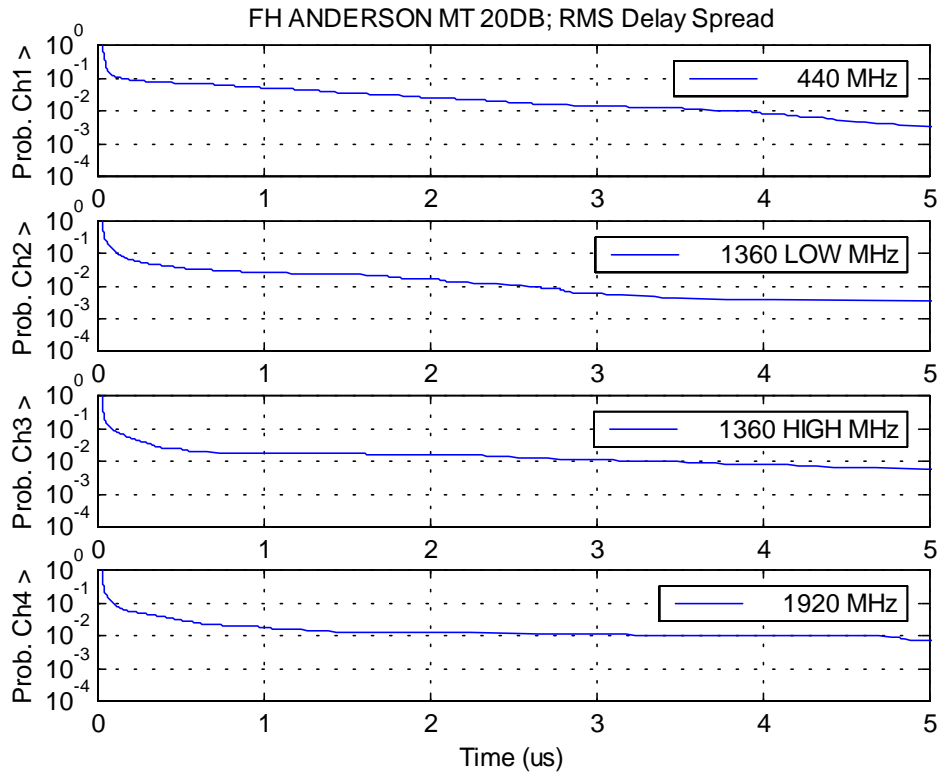
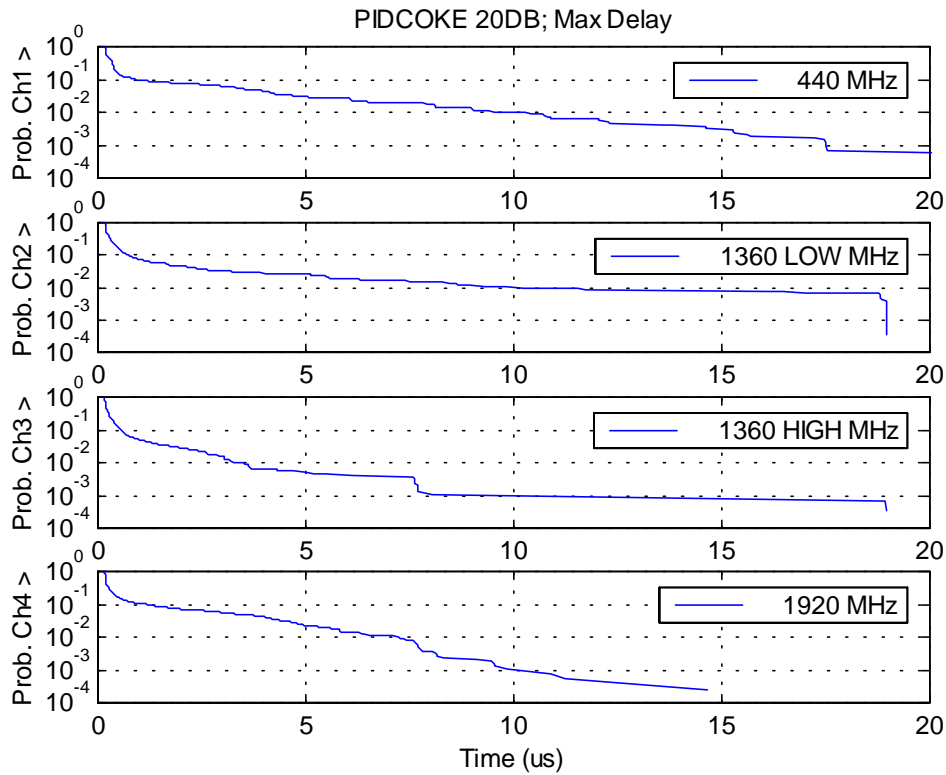Figure 5.4. Anderson Mt. 20 dB ID: RMS delay spread CDF.
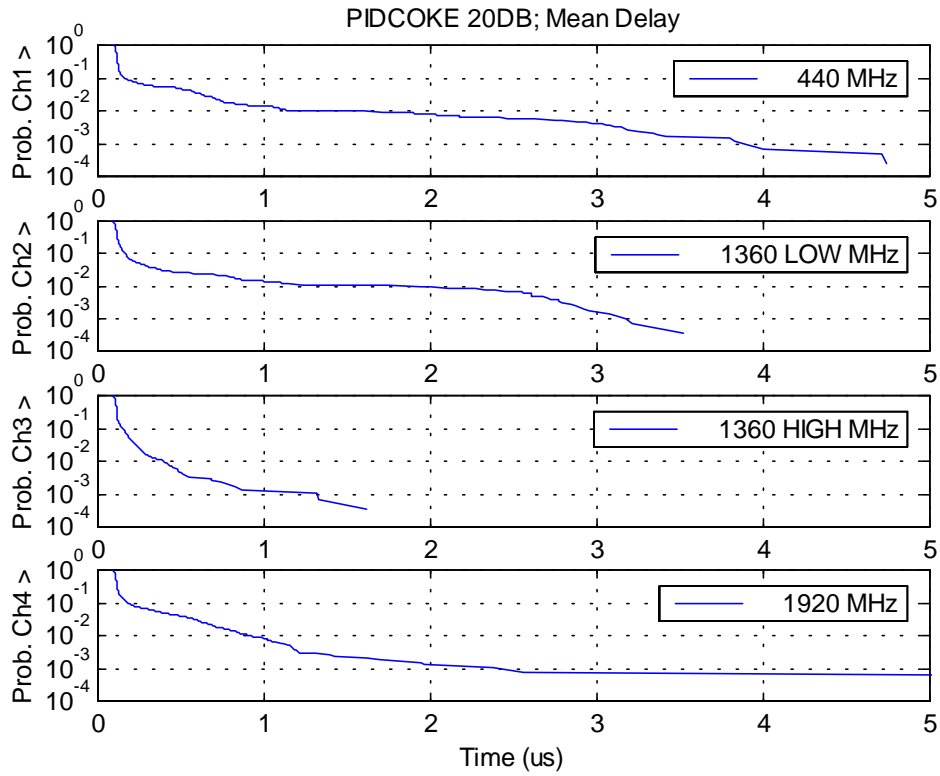

Figure 5.5. Pidcoke 20 dB ID: maximum delay CDF.

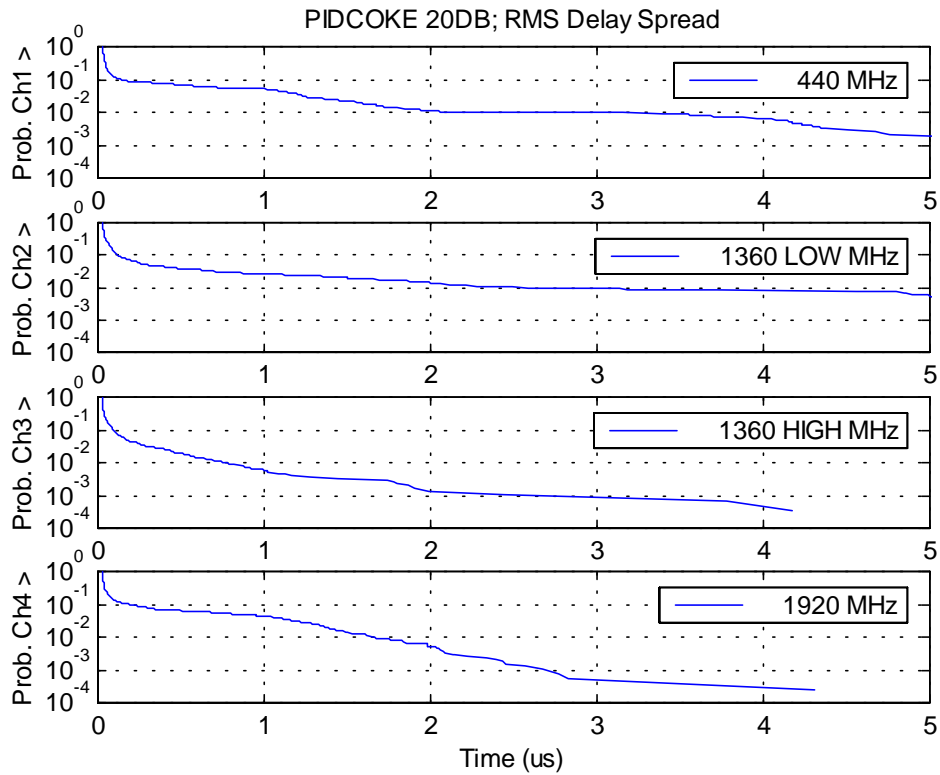Figure 5.6. Pidcoke 20 dB ID: mean delay CDF.

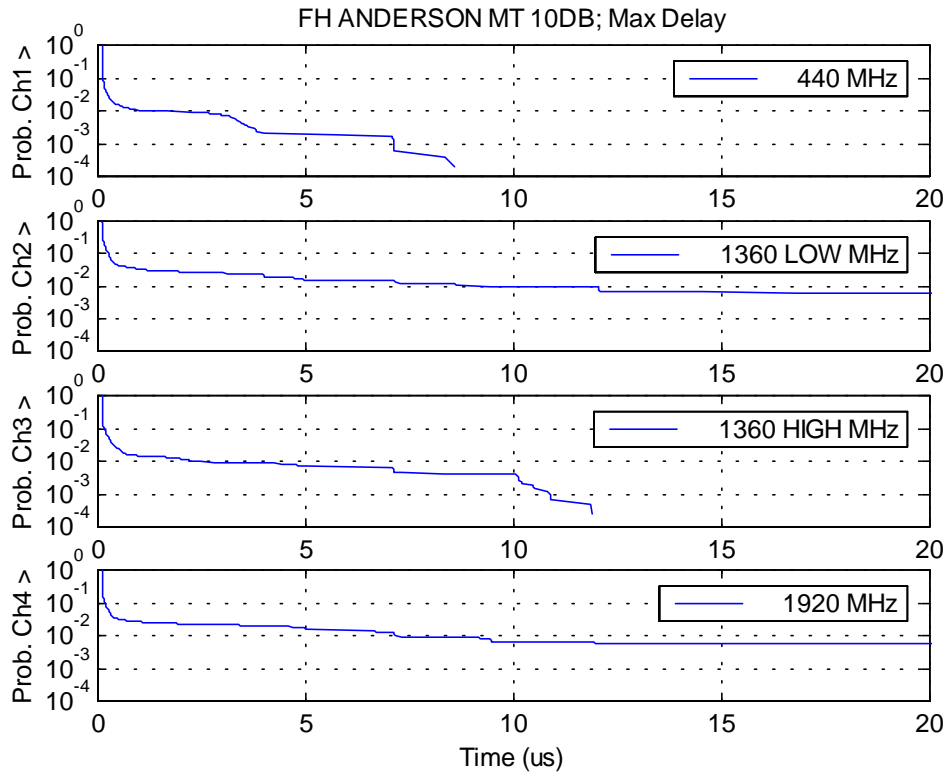Figure 5.7. Pidcoke 20 dB ID: RMS delay spread CDF.

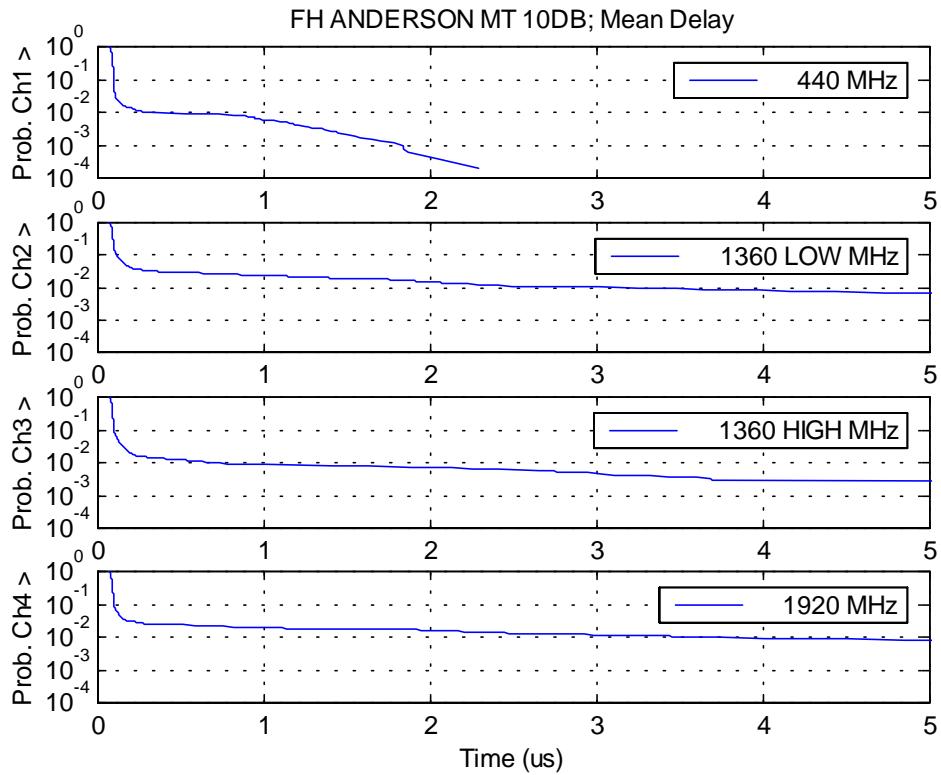Figure 5.8. Anderson Mt. 10 dB ID: maximum delay CDF.

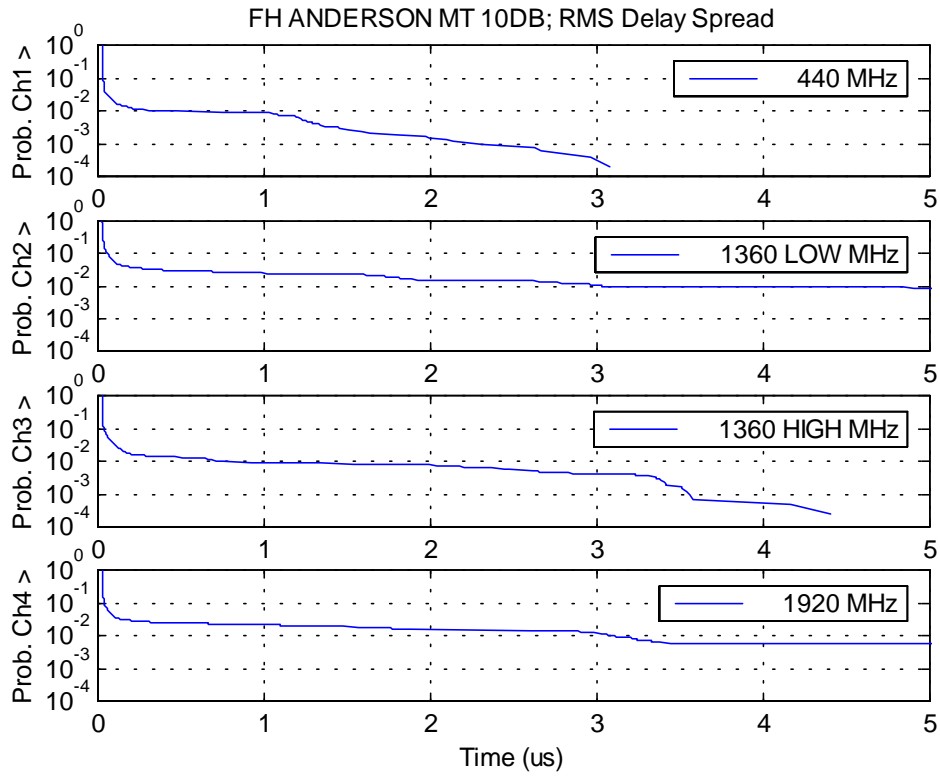Figure 5.9. Anderson Mt. 10 dB ID: mean delay CDF.

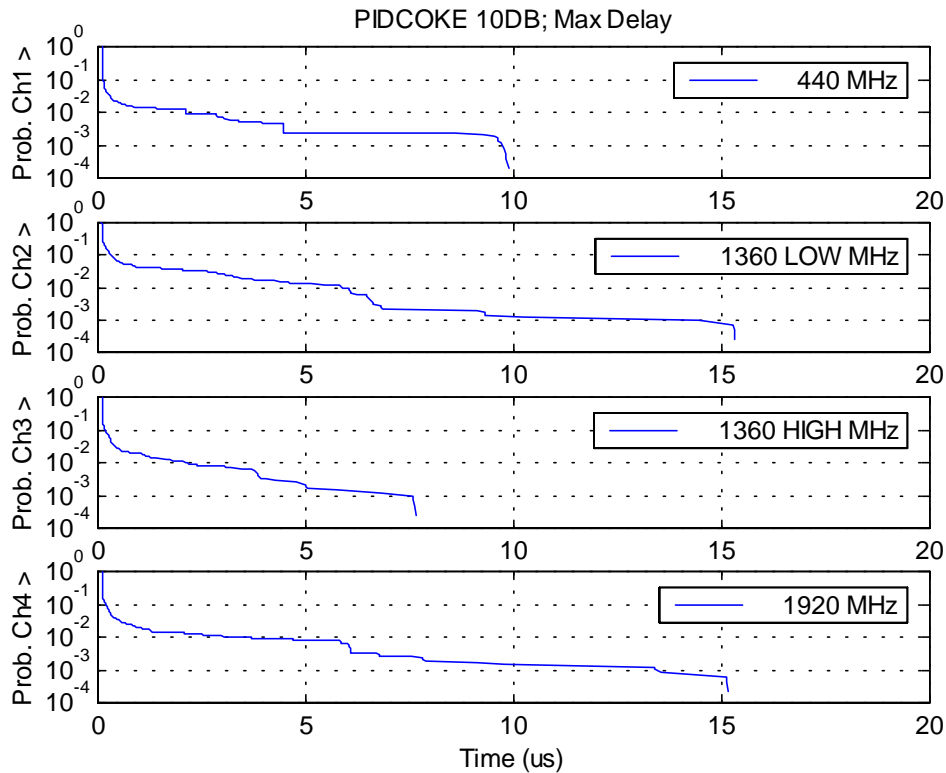Figure 5.10. Anderson Mt. 10 dB ID: RMS delay spread CDF.

Figure 5.11. Pidcoke 10 dB ID: maximum delay CDF.
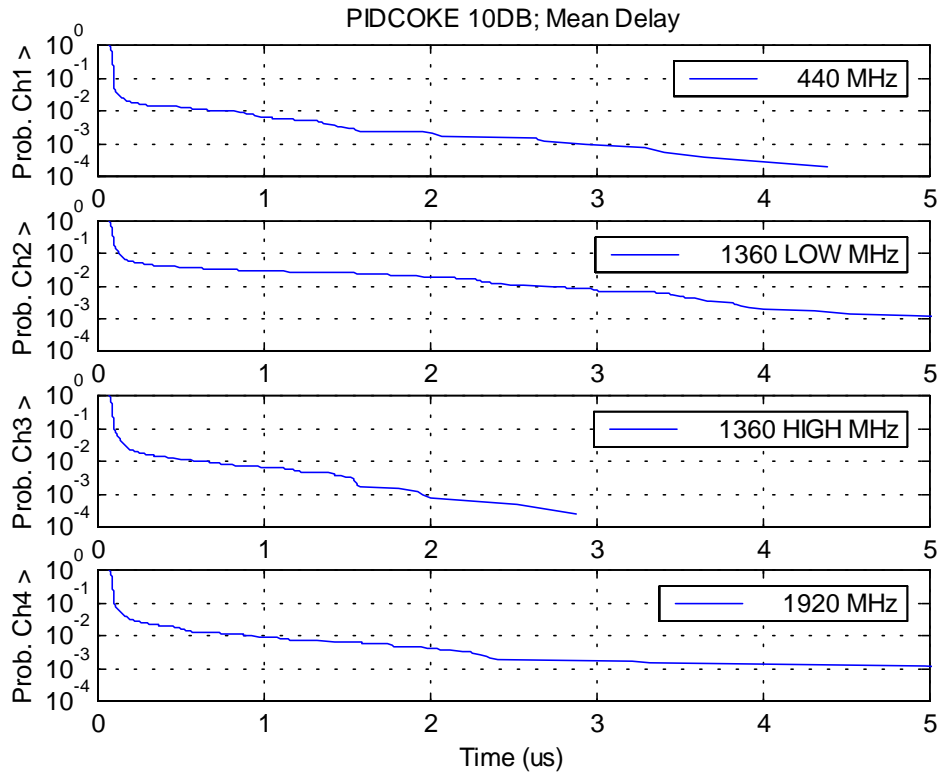
Figure 5.12. Pidcoke 10 dB ID: mean delay CDF.
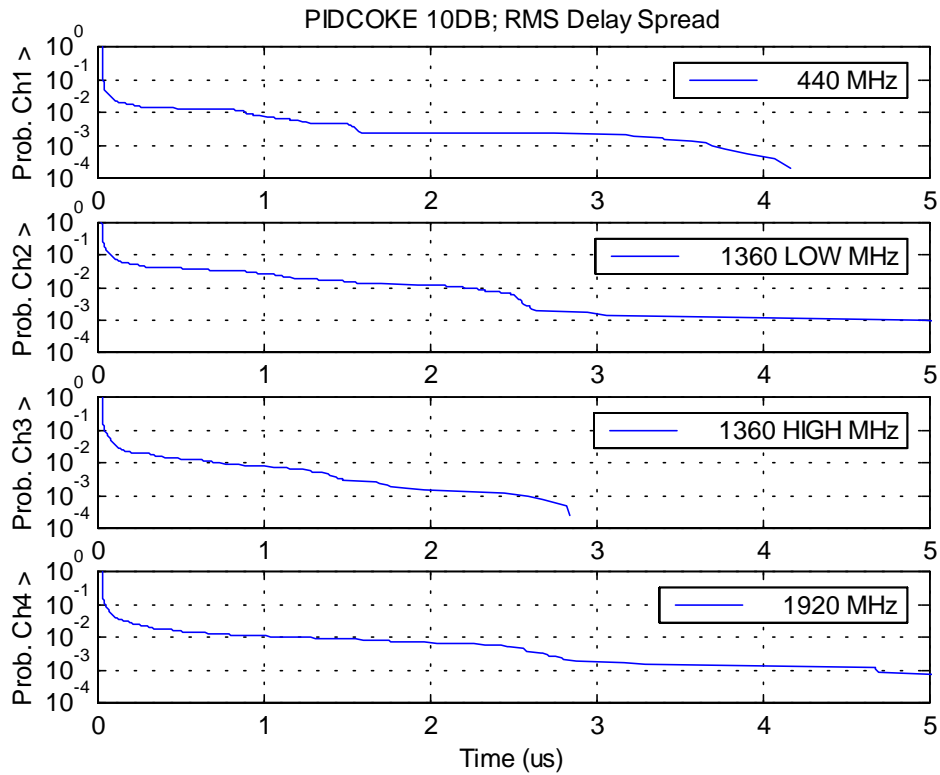
Figure 5.13. Pidcoke 10 dB ID: RMS delay spread CDF.

Figure 5.14. Delay spread (S) map, 440 MHz, Anderson Mountain transmitter site.
Figure 5.15. Delay spread (S) map, 1360 MHz (low antenna), Anderson Mountain
transmitter site.

Figure 5.16. Delay spread (S) map, 1360 MHz (high antenna), Anderson Mountain transmitter site.

Figure 5.17. Delay spread (S) map, 1920 MHz, Anderson Mountain transmitter site.

Figure 5.18. Delay spread (S) map, 440 MHz, Pidcoke transmitter site.
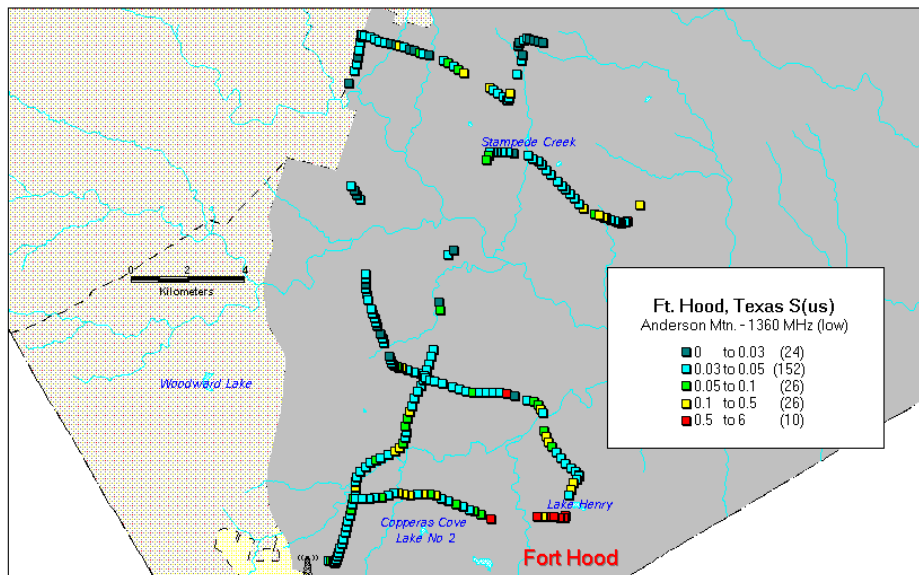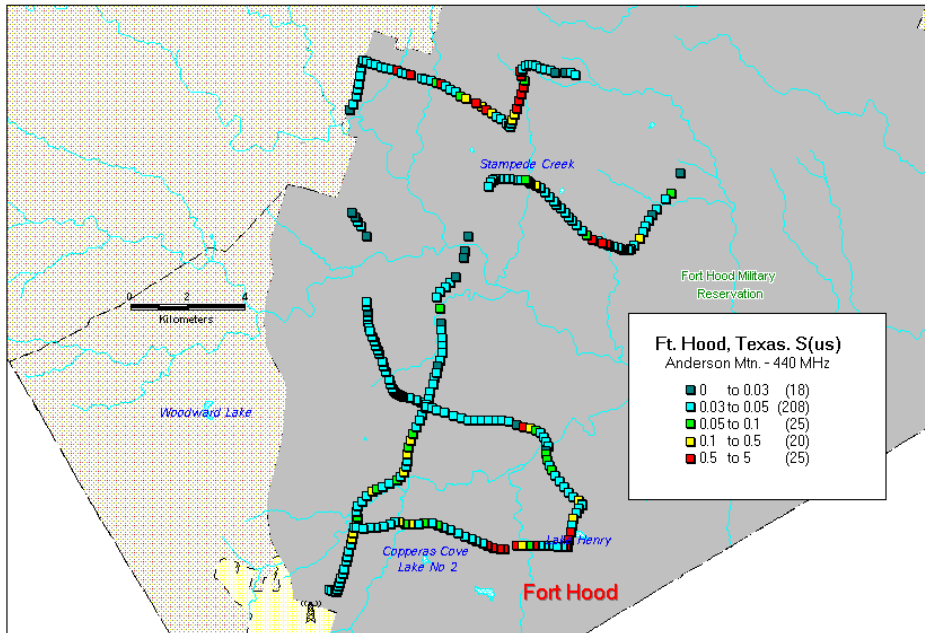Figure 5.19. Delay spread (S) map, 1360 MHz (low antenna), Pidcoke transmitter site.
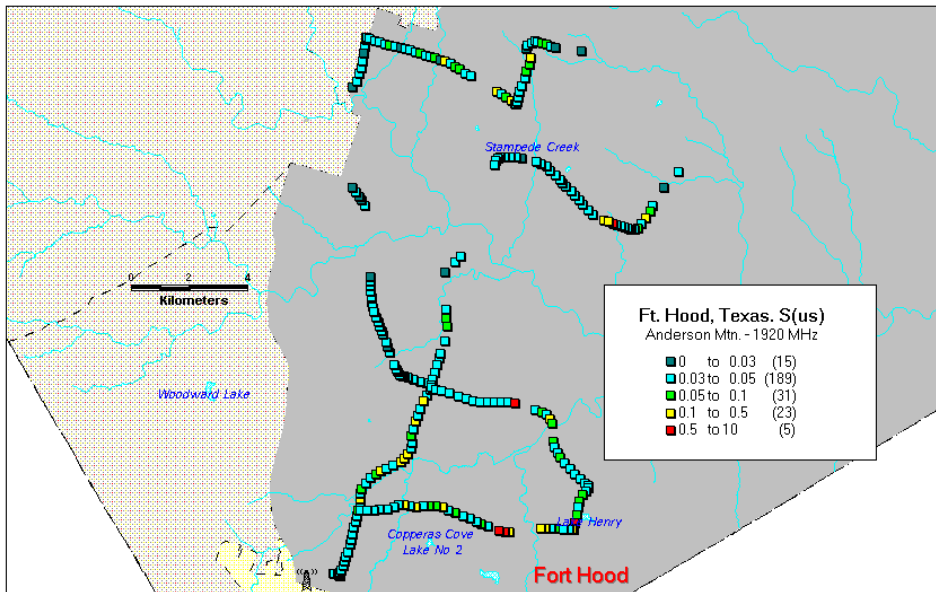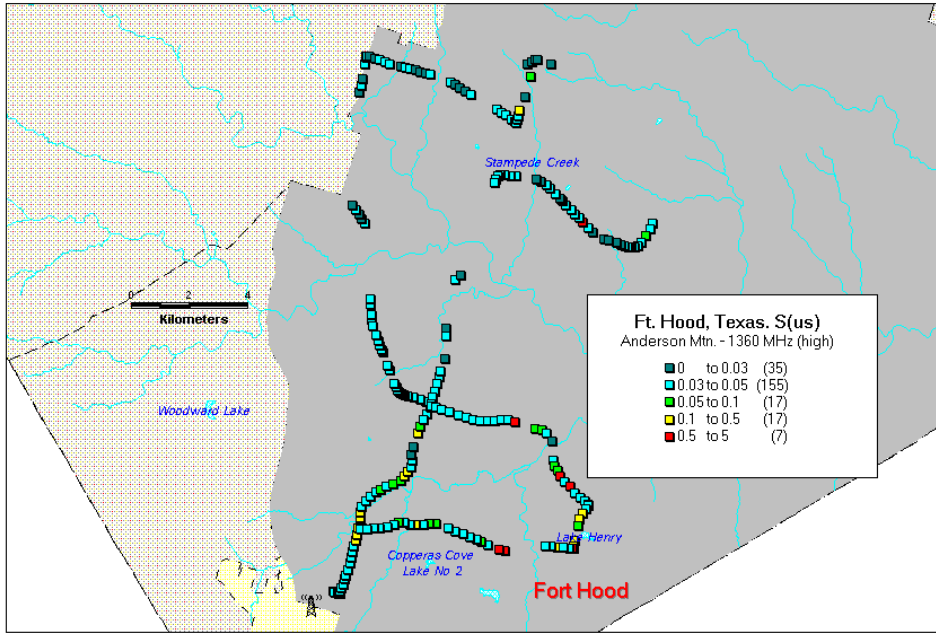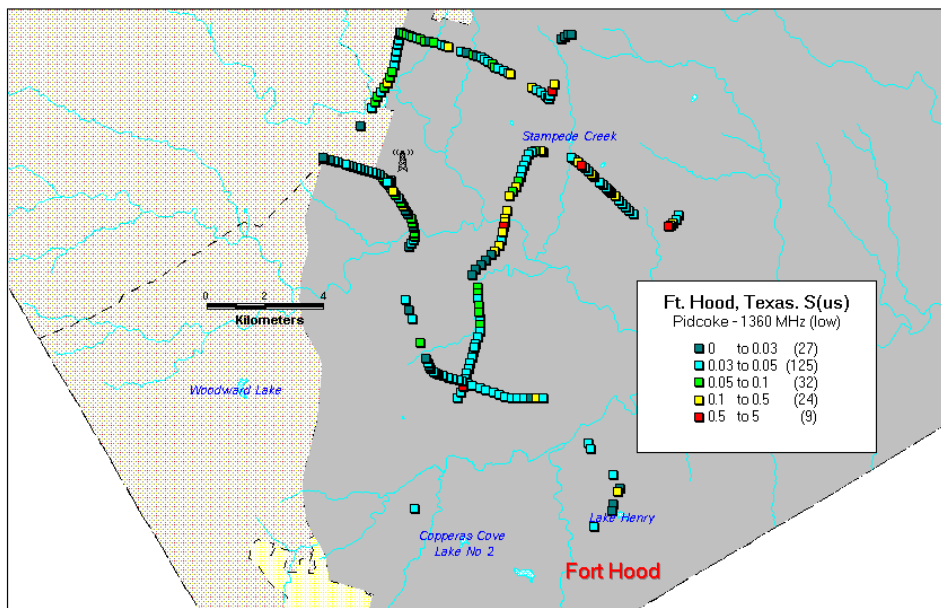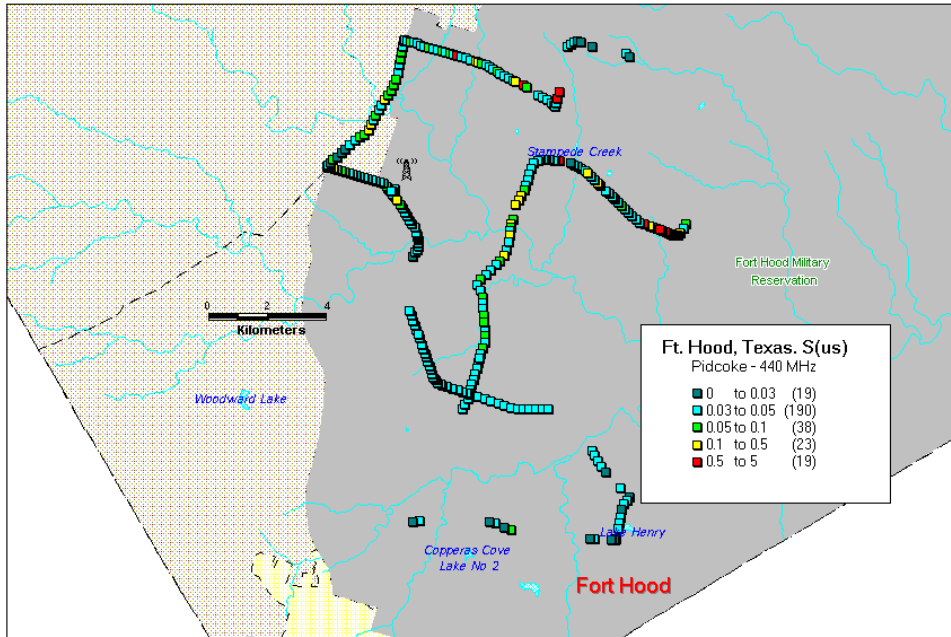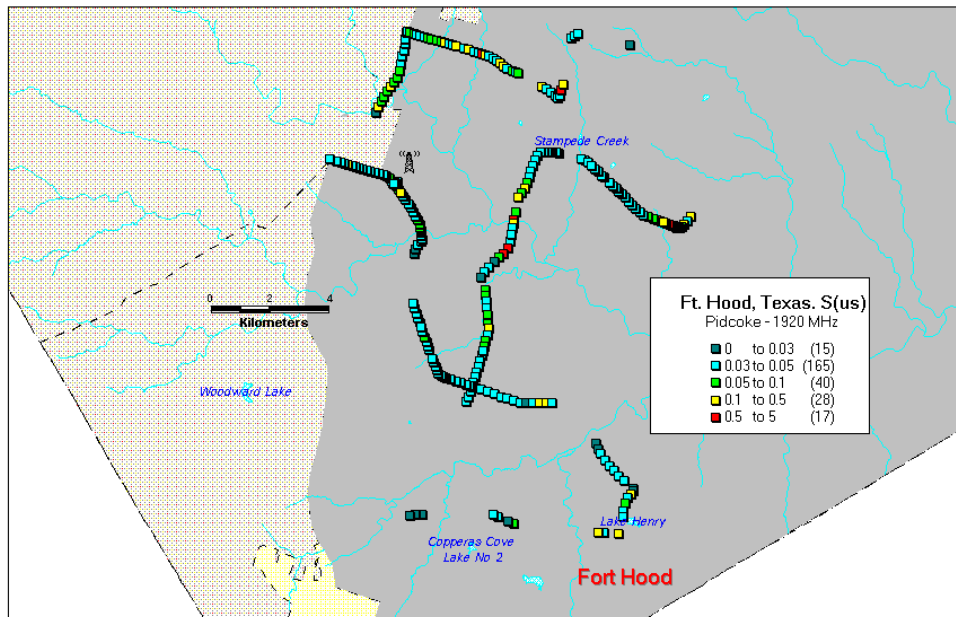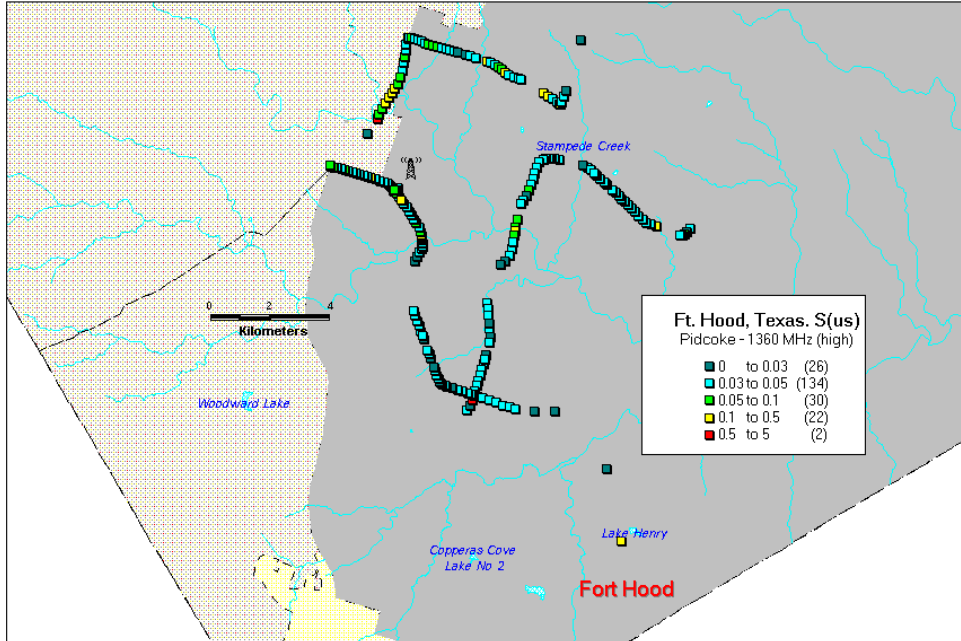
Figure 5.20. Delay spread (S) map, 1360 MHz (high antenna), Pidcoke transmitter site.
Figure 5.21. Delay spread (S) map, 1920 MHz, Pidcoke transmitter site.

APPENDIX A: ANTENNA CALIBRATION

The transmitter and receiver antennas were calibrated in a variety of environments. This is especially important for the receive antennas, which were inexpensive monopoles with limited calibration data available from the manufacturer's. The 440 MHz transmit dipole also had poor calibration data. The 1360 MHz and 1920 MHz transmit dipole antennas were high quality and had manufacturers calibration data which agree with our measurements. Calibrations consisted of two far-field tests which included the measurement vehicle and a third test which utilized the NIST anechoic chamber. The NIST test used a circular ground plane for the monopole antennas.

The first far-field test utilized a calibrated EMCO horn antenna for the 1360 MHz and 1920 MHz source and a calibrated Antenna Specialists discone antenna at 440 MHz. The source antenna gains are listed in Table A1.

Table A1. Source Antenna Gain Data used for the Far-Field Tests

Frequency(MHz)	Manufacturer	Gain(dBi)
440	Antenna Specialists	14
1360	EMCO	7.5
1920	EMCO	7.8

For this test, transmit antennas were positioned on the roof of wing 4 of the Radio Building and the van was parked east of wing 2 along the south access road. The radio path is approximately 148 m and the elevation difference is 10.4 m. The van was oriented broadside to the transmit antennas at 5 sites 1 m apart. The elevation angle was approximately 4°. Measurements were made on two separate days and averaged. The azimuth pattern of the 1360 MHz transmitter dipole was also measured. Averaged gain measurements for the field trail antennas are summarized in Tables A2 and A3.

Table A2. Gain Measurements for the Receiving Antennas

Frequency(MHz)	Manufacturer	Antenna Gain(dBi) Specification	Antenna Gain(dBi) Measured
440	Larson 5/8 λ monopole	5.2	4.8
1360(low)	Larson 1/4 λ monopole	None	-3.4
1920	Andrew PCS monopole	3	.75

Table A3. Gain Measurements for the Transmitting Antennas

Frequency (MHz)	Manufacturer	Gain(dBi) Specification	Gain(dBi) Measured
440	Cushcraft FRX430 omni directional dipole	5	0.55
1360	Dorne&Margolin DM-Q130-1 directional	12	11.33
1920	Andrew PCS-0190A-006 omni directional	6.9	6.9

Pattern measurements for the D&M antenna are given in Table A4. These results agreed well with the 360° pattern supplied by the manufacturer. The manufacturer's data was used to create a lookup table.

Table A4. 1360 MHz Dorne & Margolin Gain Measurements versus Azimuth Angle

G(0°)	G(90°)	G(180°)	G(270°)
11.3 dBi	7.3 dBi	1.3 dBi	4.3 dBi

A second set of far field tests were made at the ITS Table Mountain site, where a 360° azimuth pattern measurement of the receiving antennas and measurement van combination could be made. These tests were made at three distances at an elevation angle of 0°. The source antennas used were the same as in Table A1 except for the 440 MHz measurement, which utilized the 440 MHz Cushcraft dipole. The 440 MHz source gain has been adjusted to reflect the calibration of this antenna in the NIST chamber, as reported in the last section of this appendix. The average gain measurement over all angles and distances is given in Table A5. Figure A1 is the 360° pattern showing the influence of the van and shadowing by the mast on the roof. On this plot, 0° gives results for the van pointed head on to the calibration antenna. Also included are results for a 1360 MHz trailer mounted antenna.
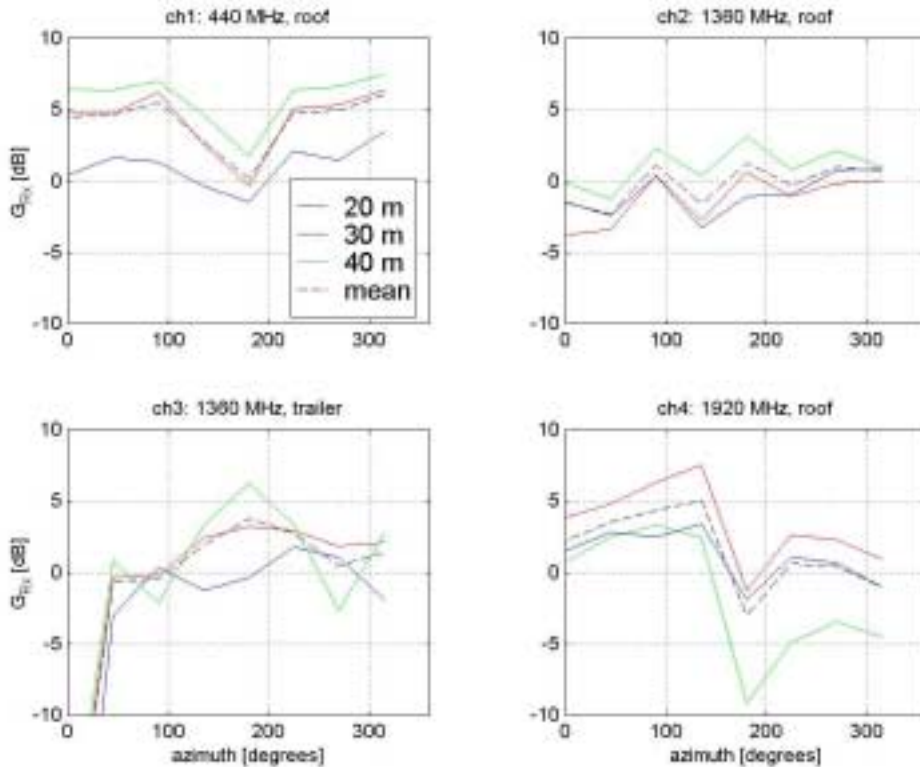
Figure A1. Antenna patterns measured at Table Mountain showing gain above isotropic versus van azimuth.

40

Antenna Pattern 440 MHz Cushcraft
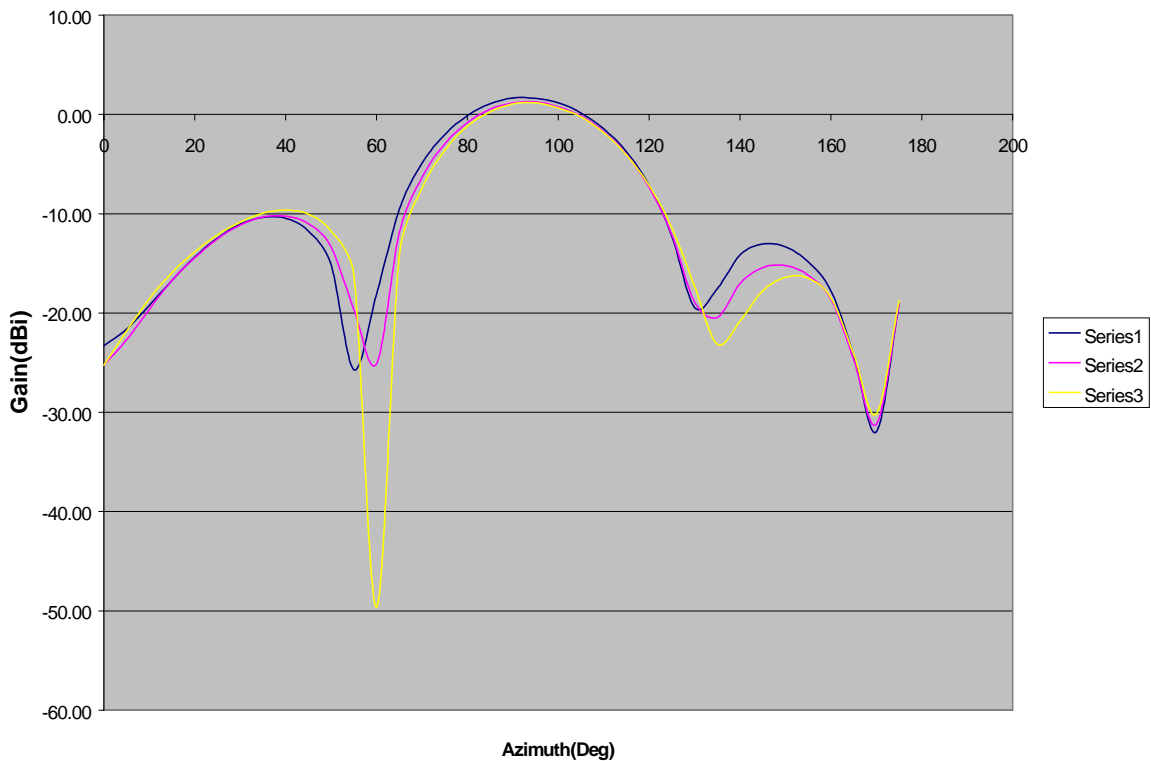
Figure A2. Gain of 440 MHz Cushcraft transmitter dipole (NIST Chamber).

Table A5. Averaged Table Mountain Azimuth Gain Measurements

Frequency(MHz)	Manufacturer	Mounting	Average Gain(dBi) Measured
440	Larson 5/8 λ monopole	Roof	4.1
1360	Larson ¼ λ monopole	Roof	-0.2
1360	Larson ¼ λ monopole	Trailer	-1.7
1920	Andrew PCS monopole	Roof	1.5

The Table Mountain measurements show the effects of the measurement van, shadowing and multipath from the ground reflection. The roof-mounted antennas were shadowed by the van mast at about 180°. This produced a 3 to 5 dB drop for about 10% of the pattern for the 440 MHz roof antenna. The 1360 MHz roof antenna has about 3-dB variability but no apparent shadowing. The 1920 MHz roof antenna has 5 to 10 dB shadowing effects for about 10% of the pattern and 3-dB variability. The 1360 MHz trailer antenna has a 10 dB drop between 0°and 20°, or about 10% of the pattern.

A third set of measurements was completed in the NIST anechoic chamber. A 1.3 m circular ground plane was utilized with the monopole receiving antennas and the vertical

pattern was measured. The vertical pattern of the 440 MHz Cushcraft transmit dipole was also measured with no ground plane. Figures A2 to A5 show the patterns for the four antennas, and Table A6 lists the measured antenna gains.

The gain of the 440 MHz Cushcraft dipole has a broad maximum near 90 degrees (on the horizon). The monopole antenna measurement plane puts 0° on the horizon. Gain for these antennas peak between 15° to 20° although the Larson 5/8 λ monopole has a broad peak near the horizon. The gain versus angle is given in Table A6.

1360 MHz Larson 1/4 wave A

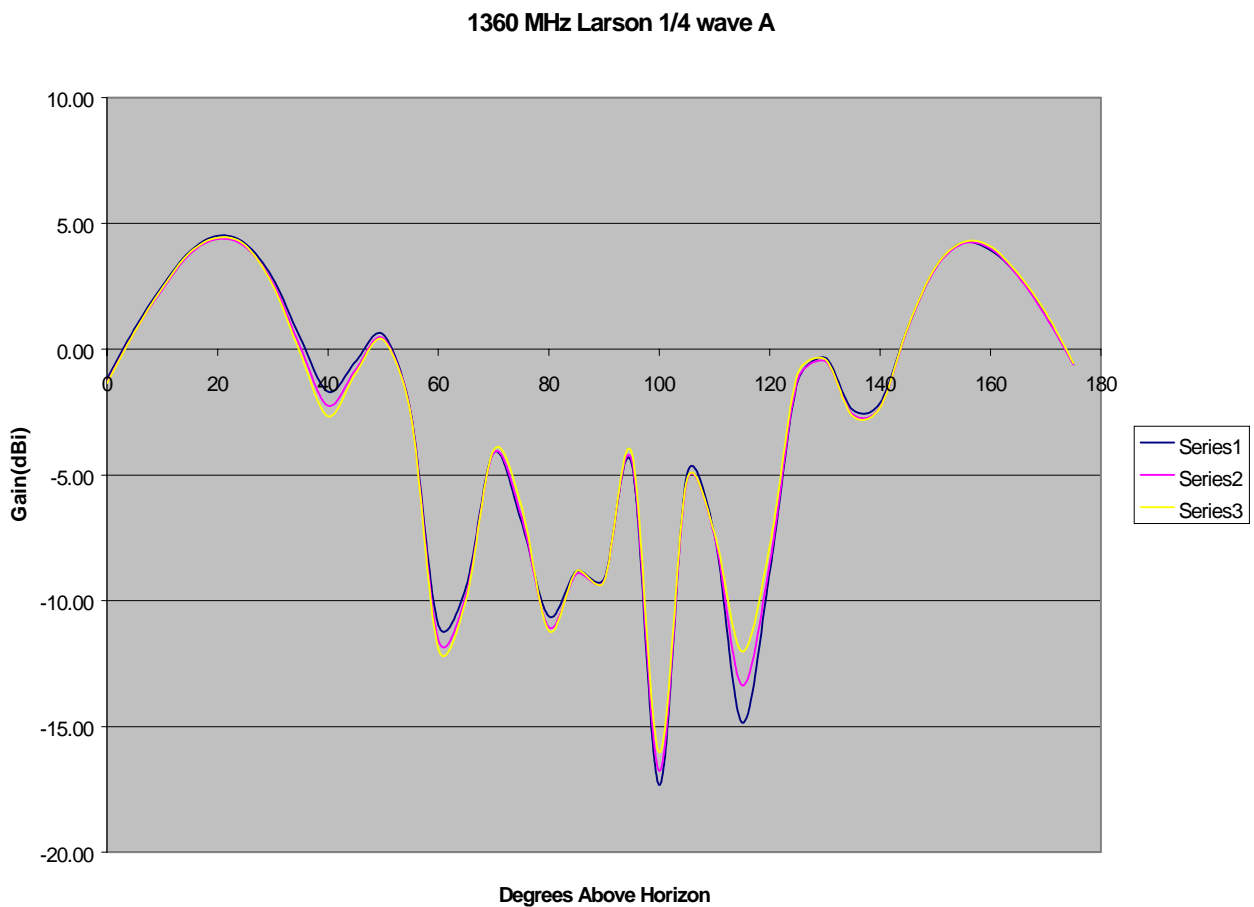Figure A3. 1360 MHz Larson receiving monopole pattern (NIST Chamber).
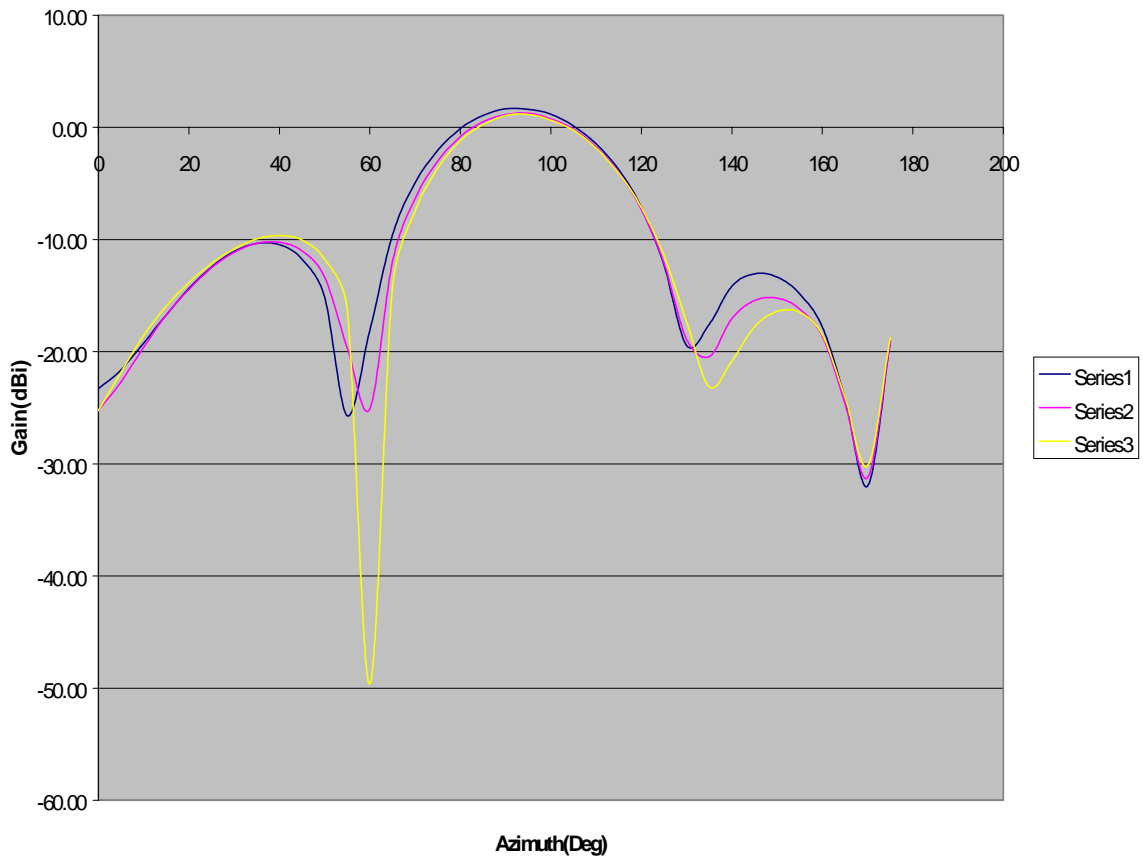
Antenna Pattern 440 MHz Cuschcraft

Figure A4. Gain of 440 MHz Cushcraft transmitter dipole (NIST Chamber).

Table A6. Gain Measured in the NIST Anechoic Chamber for the Receiving Monopole
Antennas

	Gain(dBi)											
	Larson 440 MHz			Larson 1360 MHz			Andrew 1920 MHz			Cushcraft 440 MHz		
F(MHz)	435	440	445	1355	1360	1365	1915	1920	1925	435	440	445
Elevation (deg)												
0	1.8	1.1	0.8	-1.2	-1.3	-1.4	-0.6	-0.7	-0.9	-23.3	-25.2	-25.2
5	2.4	1.9	1.6	0.8	0.7	0.7	1.5	1.4	1.2	-21.6	-22.7	-21.9
10	2.8	2.3	2.0	2.5	2.4	2.4	3.0	2.9	2.7	-19.2	-19.6	-18.6
15	2.7	2.2	2.0	3.9	3.8	3.8	3.6	3.5	3.3	-16.7	-16.7	-15.9
20	1.9	1.5	1.4	4.5	4.4	4.4	2.7	2.7	2.4	-14.4	-14.4	-13.8
25	0.5	0.1	0.1	4.2	4.1	4.1	-0.4	-0.5	-0.6	-12.4	-12.5	-12.1
30	-2.2	-2.4	-2.1	2.8	2.6	2.5	-8.0	-7.7	-7.5	-11.0	-11.1	-10.8
35	-6.3	-5.8	-5.0	0.4	0.1	-0.2	-8.5	-8.3	-8.3	-10.3	-10.3	-9.9
40	-9.7	-8.2	-6.7	-1.7	-2.3	-2.7	-3.1	-3.1	-3.2	-10.4	-10.2	-9.6
45	-6.3	-6.2	-5.5	-0.5	-0.8	-1.0	-1.7	-1.9	-2.1	-11.7	-11.0	-10.0
50	-3.4	-3.9	-3.9	0.6	0.4	0.4	-3.8	-3.9	-4.0	-15.1	-13.3	-11.7
55	-1.9	-2.8	-3.2	-2.5	-2.6	-2.6	-0.7	-0.7	-0.7	-25.7	-19.6	-16.1
60	-1.6	-2.8	-3.3	-11.0	-11.6	-11.9	-1.9	-2.2	-2.5	-18.1	-25.1	-49.6
65	-2.2	-3.5	-4.3	-9.5	-9.8	-10.0	-4.3	-4.4	-4.7	-9.6	-11.9	-14.2
70	-3.4	-4.9	-5.9	-4.1	-4.1	-4.0	-1.8	-1.7	-1.7	-4.9	-6.3	-7.4
75	-5.5	-7.0	-8.2	-6.8	-6.6	-6.2	-9.2	-9.7	-10.3	-2.0	-3.0	-3.6
80	-9.0	-10.6	-11.9	-10.6	-11.1	-11.2	-11.2	-11.6	-12.0	-0.1	-0.8	-1.2
85	-15.7	-17.6	-19.0	-8.8	-8.9	-8.8	-4.7	-4.8	-4.9	1.1	0.5	0.3
90	-22.1	-23.1	-24.1	-9.1	-9.2	-9.2	-4.3	-4.3	-4.3	1.7	1.2	1.1
95	-11.5	-12.9	-13.9	-4.5	-4.4	-4.1	-4.5	-4.4	-4.4	1.6	1.3	1.2
100	-6.9	-8.3	-9.3	-17.3	-16.8	-16.0	-11.1	-11.6	-12.2	1.2	0.8	0.7
105	-4.4	-5.6	-6.4	-5.0	-5.3	-5.2	-2.4	-2.4	-2.3	0.2	-0.2	-0.2
110	-2.8	-3.9	-4.5	-7.4	-7.4	-7.3	-2.5	-2.4	-2.5	-1.4	-1.7	-1.8
115	-2.0	-2.8	-3.1	-14.9	-13.4	-12.0	-2.1	-2.3	-2.5	-3.8	-4.0	-4.1
120	-1.9	-2.5	-2.6	-8.9	-8.5	-7.8	-0.3	-0.2	-0.2	-7.2	-7.3	-7.1
125	-2.9	-3.2	-3.0	-1.3	-1.3	-1.0	-1.4	-1.3	-1.3	-12.3	-12.1	-11.4
130	-5.3	-5.0	-4.3	-0.3	-0.5	-0.4	-0.4	-0.5	-0.7	-19.5	-18.9	-17.3
135	-9.0	-7.5	-5.9	-2.4	-2.6	-2.7	-0.6	-0.7	-0.9	-17.6	-20.4	-23.1
140	-7.7	-6.4	-5.2	-2.1	-2.3	-2.3	-4.3	-4.1	-4.0	-14.1	-17.0	-20.8
145	-3.0	-2.9	-2.5	0.9	0.8	0.9	-5.2	-4.9	-4.6	-13.1	-15.4	-17.8
150	0.1	-0.1	0.0	3.2	3.2	3.3	-0.7	-0.6	-0.6	-13.3	-15.2	-16.4
155	2.0	1.7	1.6	4.2	4.2	4.3	2.1	2.0	1.9	-14.9	-16.2	-16.5
160	3.1	2.6	2.5	3.9	4.0	4.1	3.4	3.2	3.1	-17.8	-18.6	-18.5
165	3.4	2.9	2.7	2.9	2.9	3.0	3.9	3.7	3.5	-24.3	-24.7	-24.1
170	3.3	2.7	2.5	1.3	1.3	1.4	3.8	3.7	3.5	-31.9	-31.2	-30.2
175	2.8	2.2	1.9	-0.6	-0.6	-0.6	3.0	2.9	2.8	-19.0	-19.1	-18.7

The gain on the horizon (0°) as measured in the anechoic chamber was used for data reduction. Data from the chamber for the Cushcraft 440 MHz dipole also was used. The azimuth pattern for the 1360 MHz dipole was used when reducing the data. This pattern was obtained from the manufacturer and also verified by measurements but not presented here. Table A7 and Table A8 give the gain and azimuth patterns used for data reduction.

Table A7. Receiving Antenna Gain

Receive Antenna Gains			
Frequency(MHz)	Manufacturer	Gain (dBi)	Azimuth Pattern
440	Larson	1.2	Omni
1360	Larson	-1.3	Omni
1920	Andrew	-0.7	Omni

Table A8. Transmitting Antenna Gain

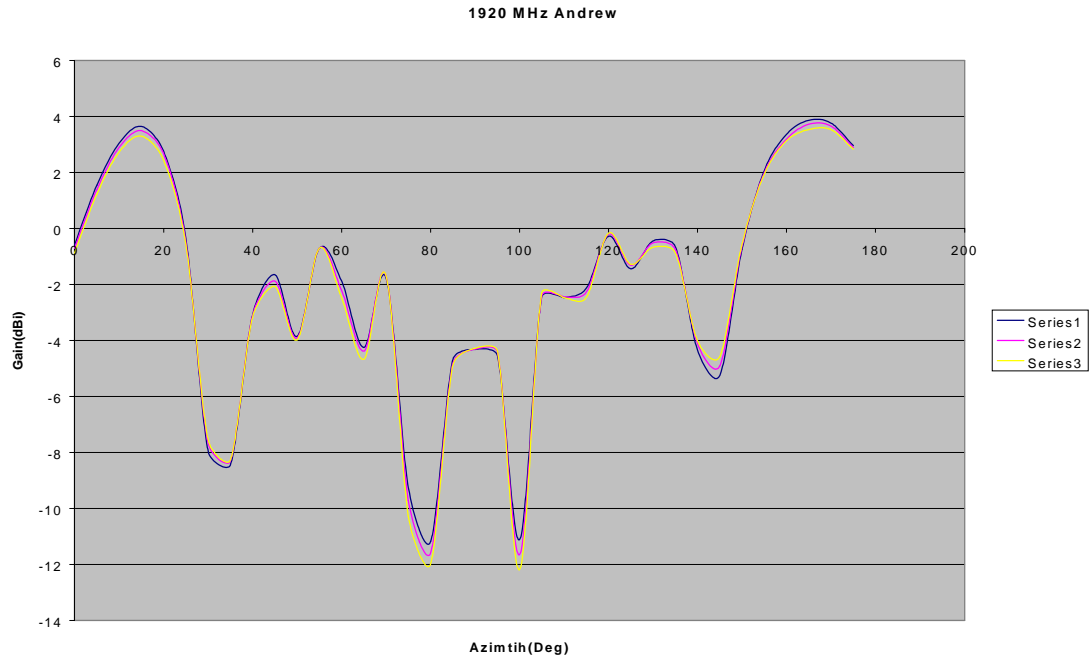| Transmit Antenna Gains			
Frequency(MHz)	Manufacturer	Gain (dBi)	Azimuth Pattern
440	Cushcraft	1.7	Omni
1360	Dorne&Margolin	11.3	Table Lookup
1920	Andrew	6.9	Omni

Figure A5. 1920 MHz Andrew receiving monopole (NIST Chamber).

45

This Page Intentionally Left Blank

This Page Intentionally Left Blank

APPENDIX B: EIRP, ANTENNA GAINS AND SITE COORDINATES

The transmitter effective isotropic radiated power (EIRP) is summarized in Table B1. Tables B2 and B3 summarize the antenna gains. Tables B3 and B4 give the GPS coordinates of the transmitter sites and the pointing angle for the 1360 MHz directional transmit antenna.

Table B1. EIRP Transmitted at Ft Hood, Texas

Cell 1 Transmitter EIRP 5/4/99			
F(MHz)	P_{TX}(dBm)	$G_{TxAntenna}$ (dBi)	EIRP(dBm)
440	35.0	1.7	36.7
1360	34.0	11.3	45.3
1920	35.3	6.9	42.2
Cell 2 Transmitter EIRP 5/5/99			
F(MHz)	P_{TX}(dBm)	$G_{TxAntenna}$ (dBi)	EIRP(dBm)
440	35.7	1.7	37.4
1360	34.6	11.3	45.9
1920	36.3	6.9	43.2

Table B2. Receiving Antenna Gain Summary

Receive Antenna Gains			
Frequency(MHz)	Manufacturer	Gain (dBi)	Azimuth Pattern
440	Larson	1.2	Omni
1360	Larson	-1.3	Omni
1920	Andrew	-0.7	Omni

Table B3. Transmitter Antenna Gain Summary

Transmit Antenna Gains			
Frequency(MHz)	Manufacturer	Gain (dBi)	Azimuth Pattern
440	Cushcraft	1.7	Omni
1360	Dorne&Margolin	11.3	Table Lookup
1920	Andrew	6.9	Omni

Table B4. Transmitter Site Coordinates (NAD83/WGS84)

Site	Latitude °N	Longitude °W
Anderson Mountain	31.13698	-97.89067
Pidcoke	31.26192	-97.87958

Table B5. 1360 MHz Transmit Antenna Pointing Angle

Site	Main Beam Boresight Angle
Anderson Mountain	N6°E
Pidcoke	E